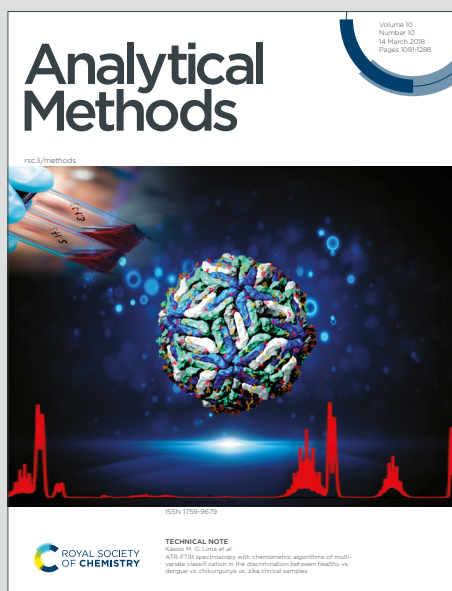


Analytical Methods

Accepted Manuscript

This article can be cited before page numbers have been issued, to do this please use: L. Feng, M. Zhang and Z. Fan, *Anal. Methods*, 2024, DOI: 10.1039/D4AY01184H.



This is an Accepted Manuscript, which has been through the Royal Society of Chemistry peer review process and has been accepted for publication.

Accepted Manuscripts are published online shortly after acceptance, before technical editing, formatting and proof reading. Using this free service, authors can make their results available to the community, in citable form, before we publish the edited article. We will replace this Accepted Manuscript with the edited and formatted Advance Article as soon as it is available.

You can find more information about Accepted Manuscripts in the [Information for Authors](#).

Please note that technical editing may introduce minor changes to the text and/or graphics, which may alter content. The journal's standard [Terms & Conditions](#) and the [Ethical guidelines](#) still apply. In no event shall the Royal Society of Chemistry be held responsible for any errors or omissions in this Accepted Manuscript or any consequences arising from the use of any information it contains.

1
2
3 **1 Current trends in colorimetric biosensors using nanozymes for detecting biotoxins**
4
5 **2 (bacterial food toxins, mycotoxins, and marine toxins)**
6
7

8
9 **3 Li Feng^{a, *}, Mingcheng Zhang^b, Zhiyi Fan^c**

10
11 **4 *a, b, c Jiyang College, Zhejiang A&F University, Zhuji Zhejiang 311800, China***
12
13

14 *** Corresponding authors: Li Feng, E-mail: lifeng@zafu.edu.cn**
15
16
17
18
19

Analytical Methods Accepted Manuscript

1
2
3
4
5
6
7
8
9
10
11
12
13
14
15
16
17
18
19
20
21
22
23
24
25
26
27
28
29
30
31
32
33
34
35
36
37
38
39
40
41
42
43
44
45
46
47
48
49
50
51
52
53
54
55
56
57
58
59
60

This article is licensed under a Creative Commons Attribution-NonCommercial 3.0 Unported Licence.
Open Access Article. Published on 09/10/2024. Downloaded on 09/10/2024. This article is licensed under a Creative Commons Attribution-NonCommercial 3.0 Unported Licence.



Abstract:

Biotoxins, predominantly bacterial food toxins, mycotoxins, and marine toxins, have emerged as major threats in seafood, food, feed, and medicine fields. They have potential teratogenic, mutagenic, and carcinogenic effects on humans, occasionally triggering high morbidity and mortality. One of the apparent concerns relates to the increasing consumption of fast food the demand for processed food without adequate consideration of the toxins they may contain. Therefore, developing improved methods for detecting biotoxins is of paramount significance. Nanozymes, a type of nanomaterials exhibiting enzyme-like activity, are increasingly being recognized as viable alternatives to natural enzymes owing to their benefits, such as customizable design, controlled catalytic performance, excellent biocompatibility, and superior stability. The remarkable catalytic activity of nanozymes has led to their broad utilization in the development of colorimetric biosensors. This has emerged as a potent and efficient approach for rapid detection, enabling the creation of innovative colorimetric sensing methodologies through the integration of nanozymes with colorimetric sensors. In this review, recent development in nanozyme research and its application in colorimetric biosensing of biotoxins is examined with an emphasis on their characteristics and performance. The study particularly focused on the peroxidase (POD) activity, oxidase (OXD) activity, superoxide dismutase (SOD), and catalase (CAT) activity of nanozymes in colorimetric biosensors. Ultimately, the challenges and future prospects of these assays are explored.

Keywords: Nanozymes; Colorimetric biosensing; Biotoxins; Food safety

1
2
3
4
5
6
7
8
9
10
11
12
13
14
15
16
17
18
19
20
21
22
23
24
25
26
27
28
29
30
31
32
33
34
35
36
37
38
39
40
41
42
43
44
45
46
47
48
49
50
51
52
53
54
55
56
57
58
59
60


Open Access Article. Published on 20/04/2024. Downloaded on 20/04/2024 14:22:04.
This article is licensed under a Creative Commons Attribution-NonCommercial 3.0 Unported Licence.



43	Table of Contents	
44	1. Introduction.....	4
45	2. Classification of nanozymes	8
46	2.1. Carbon-based nanozymes	8
47	2.2. Metal-based nanozymes	11
48	2.3. Metal oxidize-based nanozyme.....	13
49	2.4. MOF-based nanozymes.....	14
50	3. Colorimetric biosensor using nanozymes activity	16
51	2.1. POD-like activity	17
52	2.2. Oxidase-like activity	20
53	2.3. Catalase-like activity.....	25
54	2.4. Multi-enzyme-like activity.....	25
55	4. The application of nanozyme based on the colorimetric biosensor for biotoxins detection	26
56	4.1. Mycotoxins detection.....	27
57	4.1.1. Aflatoxin.....	27
58	4.1.2. Ochratoxin A	36
59	4.2. Marine toxins detection.....	40
60	4.3. Bacterial food toxins	43
61	5. Theranostic applications of nanozymes for biotoxins	47
62	6. Conclusions and future perspectives	49
63	Acknowledgments	51
64	References.....	51

1
2
3
4
5
6
7
8
9
10
11
12
13
14
15
16
17
18
19
20
21
22
23
24
25
26
27
28
29
30
31
32
33
34
35
36
37
38
39
40
41
42
43
44
45
46
47
48
49
50
51
52
53
54
55
56
57
58
59
60

Open Access Article. Published on 20/04/2024. Downloaded on 20/04/2024. This article is licensed under a Creative Commons Attribution-NonCommercial 3.0 Unported Licence.



68 1. Introduction

69 Nowadays, there is an emerging concern regarding the rapid monitoring of biotoxin presence in
70 food products^{1, 2}. Biotoxins are frequently found in bacteria, viruses, fungi, protozoa, rickettsiae,
71 and infectious substances international polluting feed, food, condiments, seafood, and so forth.
72 Biotoxins pose a risk to public health through the food chain by inducing both chronic and acute
73 toxicity, as well as exhibiting carcinogenic, teratogenic, and mutagenic impacts on human health³⁻
74 ⁵. Certain biotoxin carriers and producers menace human health and pollute the environment; they
75 can lead to crop failures and diminish the quality of agricultural products. Marine are categorized
76 based on their carriers as ciguatoxins, shellfish toxins, mytilotoxin, tetrodotoxins, and others.
77 There exists a wide range of marine toxins, exceeding 1000 different types, with several dozen
78 having been effectively characterized. These toxins have the potential to infiltrate the food chain,
79 leading to human toxicosis and potentially fatal outcomes. For instance, an estimated 750-7500
80 individuals die globally because of shellfish poisoning annually ⁶. Bacterial toxins represent a
81 distinct category of biotoxins capable of inducing foodborne illnesses through the inhibition of
82 protein synthesis, leading to neurotoxic effects. The diseases are linked to the impact of bacterial
83 toxins on tissues and are associated with distinct clinical symptoms. The most lethal bacterial toxin
84 associated with food consumption is botulinum toxin, which is created by the *clostridium*
85 *botulinum*. It has been reported that 100 ng of this toxin can be fatal to humans ⁷. Mycotoxins are
86 important class of biotoxins that produced as secondary metabolites by fungi, like *Fusarium*,
87 *Aspergillus*, *Penicillium*, *Claviceps*, *Alternaria*, *Trichoderma*, *Stachybotrys*, *Verticimonosporium*,
88 *Chaetomium*, and so forth, under favorable environmental conditions⁸. The pollution can be
89 happening throughout processing, harvesting, transportation, and storage. The International
90 Agency for Cancer Research has classified mycotoxins into distinct categories according to their

1
2
3 91 capacity to trigger cancer in humans. These classifications encompass Group 1, Group 2A, Group
4
5 92 2B, Group 3, and Group 4 carcinogens. For example, AFB1 (Group 1 carcinogen aflatoxin B1) is
6
7 93 the most toxic and abundant group of mycotoxins. It has been shown to trigger lung carcinoma,
8
9 94 hepatocellular carcinoma, colon carcinoma, and gallbladder carcinoma in humans. Liver cancer
10
11 95 is caused via AFB1 in around 28.2% of individuals ⁹.


12
13 96 In recent times, biosensors have emerged as a novel method of detection with a broad spectrum of
14
15 97 applications for the timely quantitative/qualitative assessment of various biotoxins present in food
16
17 98 products¹⁰. A biosensor is a diagnostic tool that integrates three components: a biorecognition unit
18
19 99 (e.g., aptamer, enzyme, antibody, phage, cell, etc.), a transducer and a signal conversion element¹¹,
20
21 100 ¹². The biorecognition unit is employed to specifically identify the target molecule. The interaction
22
23 101 between the target molecule and the recognition unite initiates a series of physicochemical
24
25 102 interactions. This reaction is characterized by changes such as light absorption and electrical
26
27 103 signals, which form the basis for further signal transduction processes. The transducer, being the
28
29 104 most crucial component of the biosensor, is capable of converting the above physicochemical
30
31 105 alterations into quantifiable signals, thereby facilitating signal transduction. There exist various
32
33 106 types of sensors that can be classified into four main groups based on distinct signal transduction
34
35 107 methods: optical sensors, electrochemical sensors, magnetoelectric sensors, and piezoelectric
36
37 108 sensors ^{13, 14}. Among them, the optical sensor plays a crucial role in analyzing the optical signal
38
39 109 produced during the integration of the target and the recognition unite, and then through the real-
40
41 110 time conversion and signal amplification of the transducer, it will be converted into readable data
42
43 111 to realize the quantitative sensing of the target substance. Colorimetric sensing technology is a
44
45 112 quantitative optical method that relies on the correlation between the color change of a solution
46
47 113 and the concentration of the target analyte. Compared with other optical sensors, the colorimetric

Open Access Article. Published on 20/04/2024. Downloaded from https://pubs.rsc.org on 09/05/2024 14:22:04. This article is licensed under a Creative Commons Attribution 3.0 Unported Licence.




1
2
3 114 sensor has the benefits of visualization, low cost, simple operation, and could be coupled with
4
5 115 portable substrate, so the practical use is more extensive. This method provide naked-eye sensing
6
7 116 abilities (qualitative) and could be incorporated with smartphone imaging (quantitative), making
8
9 117 them well-suited for biotoxin presence detection in various foodstuffs ^{15, 16}.

10
11 118 Enzymes are regarded as one of the earliest and most frequently utilized biometric components in
12
13 119 biosensors. They have a dual role in recognizing the target substance and promoting electron
14
15 120 transfer between the substrate, thereby catalyzing the chemical reaction of the specific substrate to
16
17 121 induce corresponding signal alterations ¹⁷. Enzymes have the capacity to act as indicators for the
18
19 122 identification of particular substances, facilitating the transformation quantities of the target
20
21 123 substance into detectable signals for analytical objectives ¹⁸. As a result, the effectiveness of
22
23 124 biosensor detection is somewhat dependent on the particular enzymes employed and their
24
25 125 individual characteristics. The defects of natural enzymes like difficulty in preservation, high cost,
26
27 126 and poor stability limit their more use in biosensors. The rapid advance of enzyme-like
28
29 127 nanomaterials (also known as nanozymes) affords an innovative horizon for the choice of suitable
30
31 128 signal markers for analyte identification. Nanozymes demonstrate catalytic properties like natural
32
33 129 enzymes, allowing them to catalyze effectively even under extreme situations. This attribute
34
35 130 expands the potential uses of nanozymes in biosensing applications ^{19, 20}. The exceptional catalytic
36
37 131 efficiency of nanozymes allows them to enhance the color change of platforms, resulting in the
38
39 132 generation of light signals upon the colorimetric platforms introduction. The colorimetric
40
41 133 biosensor that utilizes nanozymes primarily depends on the catalytic capabilities of the nanozymes
42
43 134 to imitate the natural enzymes catalytic functions. This mechanism entails the conversion of a
44
45 135 colorless substrate into a colored product through oxidation, enabling visual detection. In contrast
46
47 136 to colorimetric biosensors lacking nanozymes, the integration of nanozymes with colorimetric
48
49
50
51
52
53
54
55
56
57
58
59
60

Open Access Article. Published on 09/10/2024. Downloaded on 09/10/2024 14:22:04.
This article is licensed under a Creative Commons Attribution-NonCommercial 3.0 Unported Licence.


1
2
3 137 biosensors could serve as a means of signal amplification to a certain extent, thereby enhancing
4
5 138 the determination capabilities of biosensors ²¹. Nanozymes have the potential to serve as
6
7 139 recognition units for target analytes in biosensing systems, and their specific surface area offers
8
9 140 more active sites to bind more targets, which could further enhance the sensitivity of colorimetric
10
11 141 sensors. Furthermore, nanozymes do not possess inherent light-absorbing properties in
12
13 142 colorimetric biosensors. However, upon the addition of a colorimetric substrate, nanozymes
14
15 143 exhibit various mimetic enzyme activities that facilitate the catalysis of the substrate reaction,
16
17 144 thereby initiating a light signal. This process contributes to signal amplification in colorimetric
18
19 145 sensors²². As well, the surface properties and specific structure of nanozymes enable them to
20
21 146 function as adsorbents for selectively adsorbing target molecules. This capability can enhance the
22
23 147 selectivity of the colorimetric sensor.
24
25 148 By now, nanozyme-enabled colorimetric biosensors have been broadly employed in food safety
26
27 149 analysis owing to the advantages of naked-eye visibility, high sensitivity, easy operation, and
28
29 150 portability. However, the applications of nanozyme-enabled colorimetric biosensors in the field of
30
31 151 biotoxins analysis have not been specially summarized. Therefore, in this review, we focus on the
32
33 152 classification of nanozymes according to the different nanomaterials and offer a detailed
34
35 153 description of each type of nanozymes. Moreover, we tried to discuss the construction approach
36
37 154 of nanozymes in colorimetric biosensor in terms of catalytic activity, and affords a comprehensive
38
39 155 review of the recent research progress of nanozymes in the colorimetric biosensing various
40
41 156 biotoxin (mycotoxins, marine toxins, and bacterial food toxins) in food products. Finally, main
42
43 157 challenges and prospects of nanozyme-enabled colorimetric biosensors are also deliberated.
44
45
46
47
48
49
50
51
52
53
54
55
56
57
58
59
60

Open Access Article. Published on 09/10/2024. Downloaded on 09/10/2024 14:22:01.
This article is licensed under a Creative Commons Attribution-NonCommercial 3.0 Unported Licence.



158 2. Classification of nanozymes

159 Based on their functional activities, nanozymes can be classified into two primary groups: the
160 oxidoreductase family and the hydrolase family. The oxidoreductases predominantly participate
161 in redox reactions and exhibit various activities, including catalase (CAT), oxidase (OXD),
162 superoxide dismutase (SOD), and peroxidase (POD) like functions. Hydrolases play a crucial role
163 in catalyzing hydrolysis reactions and exhibit functions that are analogous to those of proteases,
164 nucleases, and phosphatases, etc²³. The constituents of nanozymes primarily consist of metals,
165 metal oxides, sulfides, salts, metal-organic frameworks (MOFs), carbon materials, and metal-
166 carbon hybrid nanocomposites²⁴⁻²⁶. Recently, studies on nanozymes have increasingly
167 concentrated on nanomaterials that possess intrinsic catalytic properties, rather than enzymes or
168 catalysts immobilized on nanomaterials. Currently, the majority of published research regarding
169 the nanozymes classification has focused on categorizing them according to their catalytic activity.
170 In order to offer further classification methods for nanozymes, this study emphasis on categorizing
171 them using different nanomaterials and analyzes the fabrication approaches of colorimetric assay
172 based on the various catalytic nanozymes activities.

173 2.1. Carbon-based nanozymes

174 Carbon-derived nanozymes, as a significant constituent of the nanozymes category, refer to
175 carbon-based nanomaterials having enzyme-like catalytic function. Owing to the benefits of
176 environmental friendliness, low cost, good biocompatibility, and easy modification, carbon-based
177 nanozymes are broadly employed in the fields like biosensing, environmental protection, food
178 safety, and disease diagnosis. Nevertheless, unlike other kinds of nanozymes, the synthesis of
179 carbon-based nanozymes mainly relies on a trial-and-error approach. This methodology results in
180 a notable level of uncontrollability in the modulation of the catalytic activity of carbon-based

1
2
3
4
5
6
7
8
9
10
11
12
13
14
15
16
17
18
19
20
21
22
23
24
25
26
27
28
29
30
31
32
33
34
35
36
37
38
39
40
41
42
43
44
45
46
47
48
49
50
51
52
53
54
55
56
57
58
59
60

Open Access Article. Published on 09/10/2024. Downloaded on 09/10/2024. This article is licensed under a Creative Commons Attribution-NonCommercial 3.0 Unported Licence.



1
2
3 181 nanozymes. Furthermore, carbon-based nanozymes exhibit a lower degree of substrate specificity
4
5 182 compared to other types of nanozymes, primarily due to the absence of substrate binding pockets.
6
7 183 Consequently, there is a necessity to advance rational design approaches aimed at addressing this
8
9 184 limitation. Extensive study into the characteristics of carbon-based nanomaterials has revealed
10
11 185 their significant potential for uses related to catalytic features. The concept of carbon-based
12
13 186 nanozymes was simultaneously introduced. The majority of carbon-based nanozymes are
14
15 187 documented to own POD-like or OXD-like function. Additionally, to enhance the catalytic
16
17 188 properties of these carbon-based nanomaterials, the incorporation of other elemental dopants is
18
19 189 often necessary. For instance, N-doped nanocarbon may hold the exceptional catalytic
20
21 190 performance²⁷. Nevertheless, the synthesis of N-doped carbon nanozymes with a high nitrogen
22
23 191 content presents challenges due to the instability of the N element at high temperatures. In 2019,
24
25 192 Wei and college utilized polyethyleneimine (PEI) as a source of carbon and nitrogen, alongside
26
27 193 montmorillonite (MMT) as a template, to synthesize a carbon-based nanozyme characterized by a
28
29 194 high nitrogen content²⁸. MMT was dispersed in an aqueous solution, after which the supernatant
30
31 195 was subjected to incubation with a polyethyleneimine (PEI) solution. The obtained solution
32
33 196 underwent freeze-drying to yield the assembled powder (MP), which was subsequently subjected
34
35 197 to carbonization and etching processes to produce nitrogen-doped carbon nanomaterials. This
36
37 198 study identified the critical factor, specifically the N doping content, that influences the catalytic
38
39 199 performance of carbon-based nanozymes, and thus was of great importance for the development
40
41 200 of carbon-based nanozymes with enhanced catalytic performance. Regardless of the significant
42
43 201 progress, the most of existing carbon-based nanozymes exhibit only a singular enzymatic activity.
44
45 202 Consequently, the development of methodologies to impart dual or multiple enzymatic activities
46
47 203 to carbon-based nanozymes is of considerable interest. In light of that, Gao's team used Pluronic
48
49
50
51
52
53
54
55
56
57
58
59
60

1
2
3 204 F127 as the soft template, and phenol, formalin and melamine as raw materials, to prepare a
4
5 205 polymer, which consequently was pyrolyzed to acquire the N-doped carbon ²⁹. The N-doped
6
7 206 carbon N-PCNSs3, prepared under optimal conditions, demonstrated a porous nanosheet
8
9 207 morphology, so enabling the substrates to diffuse into the pore to increase reaction performance.
10
11 208 Furthermore, the nitrogen content in N-PCNSs3 is significantly greater than that of other
12
13 209 comparable materials, which enhances its multi-enzymatic activities and overall catalytic
14
15 210 efficiency. As estimated, N-PCNSs3 had the POD-, OXD-, SOD-, and CAT-like activities. It is
16
17 211 evident that the catalytic function of carbon-based nanozymes is rest upon the precursor.
18
19 212 Consequently, altering the precursor may represent a viable approach for the development of high-
20
21 213 performance carbon-based nanozymes. In 2019, Choi and colleagues identified the photo-
22
23 214 responsive glucose oxidase (GOx) and POD-like activities of carbon nitride by carbonizing
24
25 215 melamine in the KCl and KOH existence ³⁰.
26
27 216 Graphene, a subclass of carbon materials, features high conductivity, large surface area, strong
28
29 217 thermal stability, and excellent transparency and thus, is deliberated a favorable candidate for
30
31 218 preparing carbon-based nanozymes ³¹. In 2015, Qu's team found the POD-like function of
32
33 219 graphene quantum dots (GQDs) containing of hydroxyl, carboxylic, and carbonyl elements, and
34
35 220 thoroughly explore the catalytic mechanism. Following the activity test, it was determined that the
36
37 221 carbonyl group serves as the active site and is responsible for determining catalytic activity. The
38
39 222 carboxylic group functions to interact with the substrate, while the hydroxyl group is opposite to
40
41 223 activity ³². To the best of our knowledge, this study explained the disturbance of surface functional
42
43 224 elements on catalytic function of carbon-based nanozymes for the first time, and thereby will lead
44
45 225 further researcher to progress the study of preparation and design of high-performance carbon-
46
47 226 based nanozymes. Nevertheless, graphene alone demonstrates minimal catalytic function.
48
49
50
51
52
53
54
55
56
57
58
59
60

1
2
3 227 Graphene, in isolation, demonstrates minimal catalytic activity³³. To enhance this activity, it is
4
5 228 necessary to employ a doping strategy involving other elements such as N, P, B and S.
6
7 229 Furthermore, it is essential to optimize the doping methodology to achieve the most effective
8
9 230 coordination effects. In 2019, Lee and his colleagues introduced a series of N- and B-doped
10
11 231 reduced graphene oxide, like BN-rGO, N-rGO, B-rGO (reaction between melamine and B-rGO),
12
13 232 NB-rGO (reaction between H₃BO₃ and N-rGO), and h-BN-rGO (reaction between H₃BO₃,
14
15 233 melamine, and rGO)³⁴. As expected, the synthesized rGO derivatives exhibited a nanosheet
16
17 234 morphology, with the doped elements being uniformly distributed throughout the rGO matrix. This
18
19 235 phenomenon may be attributed to the synergistic interaction between N and B, which notably
20
21 236 enhanced the electron transmission rate during POD-assisted reaction.

237 2.2. Metal-based nanozymes


238 Metal-based nanozymes are one of the most typical nanozymes owing to their easy synthesis and
239 stable structure. In general, metal-based nanozymes can be categorized into two primary types:
240 single-metal nanozymes and metal alloy nanozymes, which consist of multiple metal constituents.
241 Furthermore, various metal-doped materials, including metal core/shell nanostructures, have been
242 successfully synthesized³⁵. These nanozymes show diverse shapes, like nanowires, nanoflowers,
243 nanoparticles (NPs), nanosheets, and nanospheres. Various shapes can exhibit distinct catalytic
244 characteristics. Among them, precious metal NPs like gold, silver, platinum, and palladium are
245 commonly exploited in the determination of bacterial food toxins, mycotoxins, and marine toxins.
246 The synthesis techniques of metal-based nanozymes comprise photochemical, high-temperature
247 reduction, and mediated growth methods. In the experiments concerning nanozyme-assisted
248 analytes sensing, the reduction technique is primarily utilized. For instance, PtNPs were produced
249 using polyvinylpyrrolidone (PVP) as a stabilizing agent sodium and citrate as a reducing agent,

Open Access Article. Published on 09/09/2024. Downloaded on 09/09/2024 14:22:04.
This article is licensed under a Creative Commons Attribution-NonCommercial 3.0 Unported Licence.


250 whereas AgNPs were prepared using potassium hydroxide and L-tyrosine as raw materials, which
251 all have excellent peroxidase function^{36, 37}. In addition to exhibiting single-enzyme-like activity,
252 certain metal-based nanozymes may also demonstrate multi-enzyme-like activity. For instance,
253 peroxidase-like and oxidase-like IrNPs were made-up based on PVP and IrCl₃·3H₂O as raw
254 materials through alcohol reduction technique^{38, 39}. The combined influence of these two activities
255 enhanced the sensitivity and selectivity of the nanozyme. Due to the synergistic interactions among
256 each component, bimetallic nano-alloys frequently exhibit enhanced catalytic behavior. Recently,
257 bimetallic nanocomposites received significant attention owing to their distinctive synergistic
258 effect and multifunction, and are extensively exploited in catalytic field. The Au-Pt nanozyme
259 demonstrated superior peroxidase-like activity compared to the Au nanozyme alone and exhibited
260 greater stability over time than horseradish peroxidase (HRP). This phenomenon can be attributed
261 to the disparity in electronegativity between Pt and Au, which facilitates the migration of electrons
262 from Pt to Au. This transfer enhances the surface electron density of Au, thereby augmenting its
263 catalytic activity⁴⁰. To mitigate costs, the copper (Cu) as an element was employed in the
264 synthesis of bimetallic nanocomposites. Ramanathan et al. investigated the process of electroless
265 deposition to facilitate the in-situ growth of Cu NPs on the surface of cotton fabrics⁴¹. The obtained
266 cotton fabrics were then submerged in water solution having AgNO₃ or HAuCl₄ or PdCl₂ or
267 H₂PtCl₆ to prepare bimetallic nanoparticles, like Cu-Ag, Cu-Au, Cu-Pd and Cu-Pt. Cu-Pt NPs
268 displayed the excellent POD-like function and highest catalytic rate. Despite the extensive research
269 conducted on metal-based nanozymes, the tendency to aggregate and the toxicity associated with
270 certain heavy metals pose significant limitations to their potential applications⁴².

1
2
3
4
5
6
7
8
9
10
11
12
13
14
15
16
17
18
19
20
21
22
23
24
25
26
27
28
29
30
31
32
33
34
35
36
37
38
39
40
41
42
43
44
45
46
47
48
49
50
51
52
53
54
55
56
57
58
59
60

Open Access Article. Published on 09/10/2024. Downloaded on 09/10/2024. This article is licensed under a Creative Commons Attribution-NonCommercial 3.0 Unported Licence.



271 2.3. Metal oxidize-based nanozyme

272 As well to metal-based nanozymes, newly, metal oxide/sulfide/salt-derived nanozymes have
273 gathered higher considerable attention because they enjoyed the merits of simple preparation steps,
274 low cost, and distinctive magnetic/dielectric/optimal features^{43,44}. Considering our understanding,
275 the frequently applied techniques mainly included sol–gel, hydrothermal reaction, atomic layer
276 deposition and air pyrolysis. Through adjusting the surface groups, structures, and categories, the
277 catalytic behavior of nanozymes along with functionality and stability can be readily controlled.
278 The pioneering research on nanozymes was documented via Yan in 2007. This study revealed that
279 Fe₃O₄ NPs exhibited POD-like activity for the first time⁴⁵. Engaging TMB, OPD and
280 diaminobenzidine (DAB) as substrates, Fe₃O₄ NPs catalyzed oxidation of them producing blue,
281 brown and orange color, on the basis of which Fe₃O₄ NPs revealed POD-like function.
282 In addition to Fe₃O₄ NPs, V₂O₅ nanocomposites were also typically used to synthesis nanozymes,
283 and till now, V₂O₅ enjoying OXD-, POD-, and dual-enzyme (GOx and POD)-like function with
284 1D and 2D morphologies are introduced. The primary instance of V₂O₅ with POD-like
285 performance was documented by Tremel's team research⁴⁶. Initially, KBrO₃ and VOSO₄ were
286 combined, after which HNO₃ was slowly added to achieve a pH of 2.0. Following this, thermal
287 treatment was conducted at 180 °C for 24 h to synthesize V₂O₅ nanocomposites. In another study,
288 Doong et al exploited the bulk V₂O₅ powder as the raw material, and using DMF to separate bulk
289 V₂O₅⁴⁷. The V₂O₅ nanosheets demonstrated significant oxidative activity, effectively catalyzing
290 the oxidation of TMB to oxTMB. In 2023, Li et al. utilized the reaction between KBrO₃ and
291 VOSO₄ to synthesize 2D V₂O₅ by optimizing the reaction conditions⁴⁸. The resulting 2D V₂O₅
292 exhibited superior POD-like activity compared to V₂O₅ with other morphologies.

1
2
3
4
5
6
7
8
9
10
11
12
13
14
15
16
17
18
19
20
21
22
23
24
25
26
27
28
29
30
31
32
33
34
35
36
37
38
39
40
41
42
43
44
45
46
47
48
49
50
51
52
53
54
55
56
57
58
59
60

Open Access Article. Published on 09/10/2024. Downloaded on 09/10/2024 14:22:04.
This article is licensed under a Creative Commons Attribution-NonCommercial 3.0 Unported Licence.




1
2
3 293 MnO₂ was also typically used to develop nanozymes with CAT-, POD-, OXD-, GO_x- and SOD-
4
5 294 like activities. For instance, Han and colleagues used BSA as soft template to controllably produce
6
7 295 2D MnO₂ nanozyme⁴⁹. Actually BSA with rich-NH₂ and -COOH elements could efficiently fixe
8
9 296 Mn²⁺ in its molecular structure to generate Mn²⁺@BSA. Upon the addition of NaOH, Mn²⁺ present
10
11 297 in the Mn²⁺@BSA complex was initially converted into MnO(OH). This intermediate
12
13 298 subsequently underwent oxidation by O₂, ultimately resulting in the formation of MnO₂. As
14
15 299 anticipated, the synthesized MnO₂ under alternative conditions exhibited an irregular flocculent
16
17 300 morphology, highlighting the significant influence of BSA.

18
19 301 To sum up, metal oxide-based nanozymes, like peroxidase-like V₂O₅, GeO₂, TiO₂, Fe₃O₄, and
20
21 302 oxidase-like MnO₂ are also employed in the determination of various toxins. Nevertheless, the
22
23 303 unmodified metal oxide-derived nanozymes might display poor stability and other challenges⁵⁰.
24
25 304 Consequently, some researchers will alter specific components within the metal oxide to enhance
26
27 305 its detection efficacy.

306 2.4. MOF-based nanozymes

307 MOFs are crystalline materials characterized by a periodic network structure that arises from the
308 self-assembly of organic components, typically organic ligands such as pyridine or carboxylic
309 acids, in conjunction with metal clusters or metal ions, predominantly comprising transition metal
310 ions like Fe²⁺, Zn²⁺, and Cu²⁺^{51, 52}. MOFs are a class of nanomaterials that have garnered
311 significant interest in recent years due to their advantageous characteristics, including a high
312 specific surface area, a porous network structure, and tunable chemical properties⁵³. The poor
313 selectivity is prevalent among numerous nanozymes; therefore, it is essential to conduct a thorough
314 investigation into the factors contributing to the high selectivity observed in natural enzymes and
315 to incorporate these insights into the development of nanozymes. Similarly, when utilizing MOF-

Open Access Article. Published on 09/11/2024. Downloaded from https://pubs.rsc.org on 09/11/2024. This article is licensed under a Creative Commons Attribution-NonCommercial 3.0 Unported Licence.



1
2
3 316 based nanozymes in vivo, it is imperative to assess their cytotoxicity and biosafety to confirm that
4
5 317 they do not pose any harm to the organism. According to their synthesis approaches, MOF-based
6
7 318 nanozymes could be divided into chemically modified MOF, pristine MOF, MOF derivatives and
8
9 319 MOF-based composites ⁵⁴.

10
11
12
13 320 The coordination binding sites of the metal centers within MOFs are often obstructed by the
14
15 321 organic moieties, leading to diminished catalytic activity. Therefore, it is imperative to explore
16
17 322 novel strategies to address this issue and enhance the catalytic performance of the unmodified
18
19 323 MOF. Strategies have been established to augment their catalytic performance, like assembly of
20
21 324 metal nanoparticles, surface modification of MOFs, metal oxides, and other constituents in MOF
22
23 325 ⁵⁵. The Fe₃O₄@MIL-100(Fe) composites were effectively synthesized using an in-situ growth
24
25 326 technique, which involved the incorporation of Fe₃O₄ NPs within the MIL-100 framework. The
26
27 327 catalytic potential of these MOF composites for photo-Fenton reactions was subsequently
28
29 328 investigated ⁵⁶. Research has also been conducted on the synthesis of AuNPs@MIL-101
30
31 329 composites through the hydrothermal deposition of AuNPs onto the MIL-101 MOF. This
32
33 330 composite material exhibits catalytic properties for the oxidation of ascorbic acid, which can be
34
35 331 utilized in conjunction with an electrochemical sensor for the detection of microcystin-LR in water
36
37 332 samples ⁵⁷. Both rGO and TiO₂ have been revealed to couple with MIL MOFs to improve their
38
39 333 catalytic function^{58, 59}. In addition, MOFs could also be applied as templates or precursors to
40
41 334 provide a series of MOF derivatives, for example carbon materials, metal oxides, metals, and so
42
43 335 on, owing to their modifiable structures. For instance, by calcining the precursors of Fe-ZIF-67
44
45 336 and Fe-ZIF-8 at high temperatures, a Fe-N-C nanozyme with POD-like function was achieved,
46
47 337 which exhibited good performance ⁶⁰.

3. Colorimetric biosensor using nanozymes activity

As is well known, colorimetric biosensing relies on the correlation between the extent of color alteration in the platform and the level of the analyte substance to enable quantitative determination. The alteration in substrate color is dependent on the catalytic function of the enzyme. Nanozymes typically facilitate the conversion of a colorless substrate into a colored one through their inherent enzyme-like properties. For instance, nanozymes exhibit the ability to induce color changes in various substrates, including OPD (o-phenylenediamine), TMB, ABTS, and other chromogenic substrates, enabling colorimetric recognition. Recently, the most research endeavors concerning the catalytic capabilities of nanozymes have primarily concentrated on imitating oxidoreductase characteristics, specifically those associated with OXD, POD, CAT, and SOD functionalities⁶¹. Some previous studies have explored hydrolytic enzyme mimics, however, the focus has shifted towards the oxidoreductase-imitating capabilities of nanozymes, particularly in the context of colorimetric sensing. This section primarily examines the development strategies and advancements in employment colorimetric nanoprobe that leverage the oxidoreductase-like properties of nanozymes. In recent years, there has been a growing interest in the integration of biosensors with innovative nanomaterials, and nanozymes are broadly exploited in colorimetric recognizing platforms owing to their superior stability and exceptional catalytic characteristics. From one perspective, nanozymes have the potential to serve as biorecognition units for analytes in biosensing applications, as they offer a large specific surface area that can render numerous active sites for binding multiple targets, which in turn can effectively boost the colorimetric sensors sensitivity^{62, 63}. Furthermore, nanozymes lack inherent light-absorbing characteristics in colorimetric nanoprobe. However, upon the addition of a colorimetric platform, nanozymes exhibit diverse simulated enzyme performances that facilitate the catalysis of the surface reaction,

1
2
3
4
5
6
7
8
9
10
11
12
13
14
15
16
17
18
19
20
21
22
23
24
25
26
27
28
29
30
31
32
33
34
35
36
37
38
39
40
41
42
43
44
45
46
47
48
49
50
51
52
53
54
55
56
57
58
59
60

Open Access Article. Published on 09/10/2024. Downloaded on 09/10/2024 14:22:04.
This article is licensed under a Creative Commons Attribution-NonCommercial 3.0 Unported Licence.



1
2
3 361 thereby initiating a light signal. This mechanism enables nanozymes to contribute to signal
4
5 362 enhancement within colorimetric probes ²². Additionally, the distinct building and interface
6
7 363 characteristics of the nanozymes enable them to function as adsorbents for selectively capturing
8
9 364 the desired molecules. This capability could enhance the colorimetric assay selectivity. More
10
11 365 importantly, nanozymes play a crucial role in inducing a color change in the substrate as part of
12
13 366 the catalytic process. This transformation enables the conversion of the concentration or amount
14
15 367 of the desired molecules into visible hue indicators, facilitating the naked eye detection of signal
16
17 368 variations through colorimetric sensors.

369 **2.1. POD-like activity**

370 Peroxidase could catalyze the reaction in the peroxides existence like ROOH and as H₂O₂ redox
371 substrates and electron acceptors, changing them to oxidation and H₂O products ⁶⁴. The
372 nanozymes' POD mimetic system exhibits ping-pong mechanism and Michaelis-Menten kinetics
373 similar to those observed in the catalytic behavior of natural peroxidase enzymes ⁶¹. The ping-
374 pong mechanism is defined by the enzyme's alternating transition between its initial conformation
375 and an altered state. This process involves the enzyme releasing the initial product upon binding
376 with the initial substrate in its base state, transitioning to the altered form, and reverting to the
377 original conformation upon binding with the second substrate to release the subsequent product ⁶⁵.
378 In contrast to the OXD mimetic activity, the POD mimetic system requires the presence of H₂O₂.
379 H₂O₂ serves as a natural scaffold toward POD, and the nanozymes facilitate the breakdown of the
380 O–O bond in H₂O₂ into (\cdot OH) with significant oxidation potential. The resulting \cdot OH species can
381 subsequently oxidize various colorimetric substrates, including OPD, ABTS, TMB, and other
382 similar compounds ²². The production of \cdot OH in processes mimicking peroxidase enzyme activity
383 has been documented through two pathways. One pathway involves the Fenton reaction, where

Open Access Article. Published on 09/10/2024. Downloaded on 20/11/2024 14:22:04. This article is licensed under a Creative Commons Attribution-NonCommercial 3.0 Unported Licence.




384 Fe^{2+} reacts with H_2O_2 to produce $\cdot\text{OH}$ and hydroxides (OH^-). The Haber-Weiss reaction as a
385 second pathway can catalyze superoxide ($\cdot\text{O}_2^-$) via iron ions and H_2O_2 leads to the generation of
386 $\cdot\text{OH}$ ⁶⁶.

387 The emerging trend in analytical chemistry involves utilizing nanozymes with inherent peroxidase-
388 like activity in conjunction with colorimetric biosensors for the purpose of detecting specific target
389 substances. This approach is using catalytic color development concept through nanozymes.
390 Graphite-like carbon nitride (g- C_3N_4) nanosheets exhibit properties similar to POD enzymes with
391 notable stability. Notably, the functionalization of g- C_3N_4 with heteroatoms has been shown to
392 substantially improve its POD-like activity. In this regard, Fu's group activated g- C_3N_4 with Pd
393 NPs for the improvement of its enzyme-catalyzed performance and loaded the heteroatom-
394 activated g- C_3N_4 with Fe_3O_4 ⁶⁷. A magnetic platform consisting of Fe_3O_4 /Pd NPs supported on g-
395 C_3N_4 was developed to enhance POD-like activity and utilized for immobilizing different natural
396 enzymes, aiming to achieve material reusability and mitigate optical nanozymes interference
397 caused by scattering in colorimetric sensors. Using Fe_3O_4 /Pd NPs/g- C_3N_4 /GOx, a colorimetric
398 probe was developed for the determination of glucose. There was no detectable evidence at 652
399 nm once TMB, glucose, and Fe_3O_4 /Pd NPs/g- C_3N_4 without GOx were existent, indicating that
400 Fe_3O_4 /Pd NPs/g- C_3N_4 does not exhibit inherent GOx-like function. The alteration in TMB hue was
401 observed only when Fe_3O_4 /Pd NPs/g- C_3N_4 /GOx, TMB, and target were co-present.

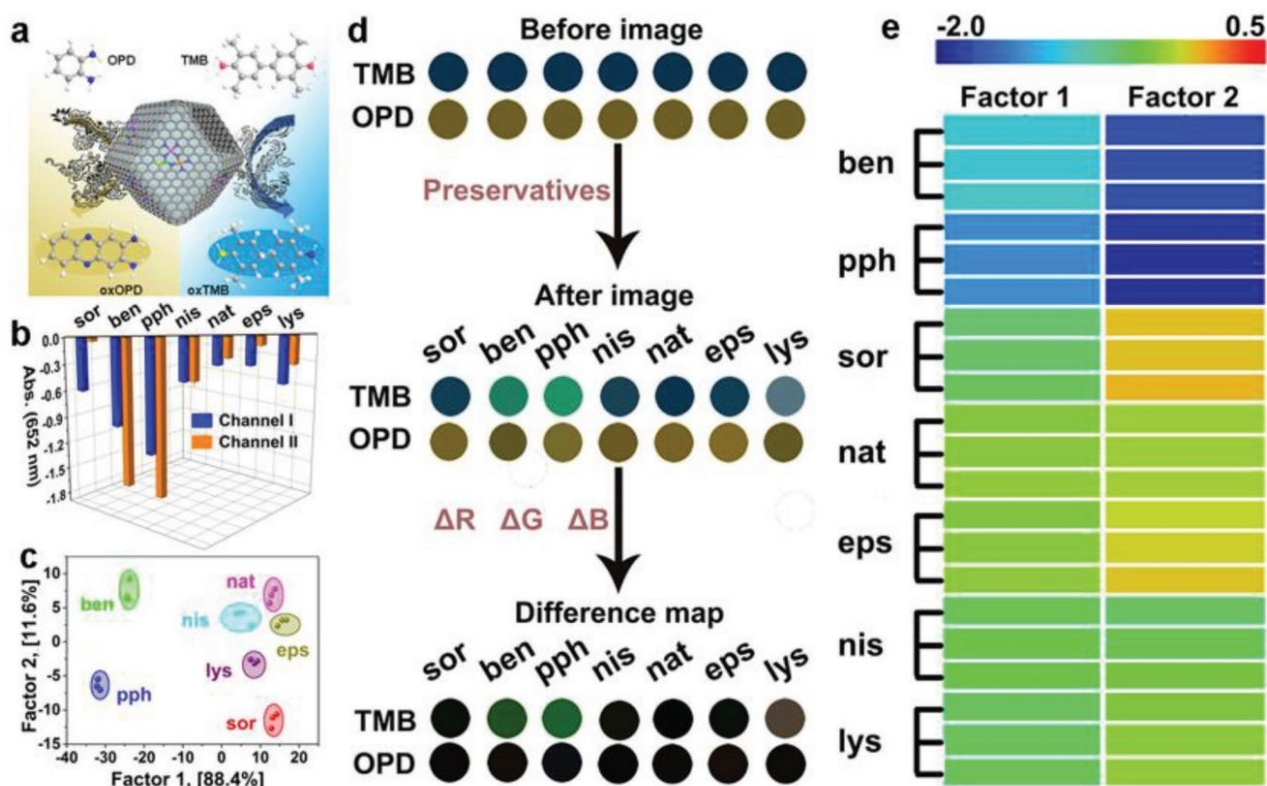
402 In another study, Li et al. ⁶⁸ produced S- and N-doped carbon-loaded POD-like FeCoZn triatomic
403 catalysts stemmed from ZIF-8 by taking benefit of two properties, specifically, that MOFs could
404 efficiently mitigate the issue of single-atom catalyst agglomeration and the potential of dispersing
405 multiple metal atoms to boost the efficiency of single-atom nanozymes. A colorimetric nanozyme
406 using dual-channel assay was developed by integrating FeCoZn-TAC/SNC with a sensor array,

1
2
3
4
5
6
7
8
9
10
11
12
13
14
15
16
17
18
19
20
21
22
23
24
25
26
27
28
29
30
31
32
33
34
35
36
37
38
39
40
41
42
43
44
45
46
47
48
49
50
51
52
53
54
55
56
57
58
59
60

Open Access Article. Published on 09/09/2024. Downloaded on 09/09/2024. This article is licensed under a Creative Commons Attribution-NonCommercial 3.0 Unported Licence.



aimed at differentiating food preservatives (Figure 1). The FeCoZn-TAC/SNC nanozymes exhibit POD-like activity, facilitating the color development reactions of TMB and OPD to yield green and yellow products, respectively. The food preservatives can adhere to the nanozyme surface via hydrogen bonding and π - π stacking interactions. The diverse levels of interaction noted between FeCoZn-TAC/SNC and different food preservatives led to a reduction in the catalytic efficiency of the nanozymes. Consequently, this occurrence resulted in varying degrees of color signals, which serve as the fundamental mechanism for discriminating among the preservatives. According to this principle, the colorimetric reaction profiles of various preservatives exhibit variations. Through linear discriminant analysis, a 100% accuracy rate was attained during the cross-validation of seven food preservatives. This result indicates that the sensor array adeptly distinguished seven varieties of food preservatives even at low concentrations.



419


420 **Figure 1.** Schematic drawing of fabricating a colorimetric biosensor using two-channel array on
421 the basis of the POD-like function of nanozymes for discriminating food preservatives. Reprinted
422 with permission from Ref ⁶⁸.

423 2.2. Oxidase-like activity

424 Oxidases have the ability to facilitate the substrates oxidation (such as electron donors) in the
425 existence of molecular oxygen or other oxidants (such as electron acceptors), leading the
426 production of oxidation products along with H₂O, H₂O₂, or O²⁻. Currently, a variety of nanozymes
427 have been identified to exhibit oxidase-like activity. Massimiliano and colleagues discovered that
428 gold nanoparticles (Au NPs), even when not loaded with protective agents, exhibited enhanced
429 catalytic activity. Bare Au NPs exhibited the capability to catalyze the production of H₂O₂ and
430 gluconate from glucose in the O₂ presence. In contrast, colloidal particles of Ag, Cu, Pt, and Pd
431 did not demonstrate comparable activity under identical conditions ⁶⁹. Thereafter covalent organic
432 frameworks, metal-organic frameworks, carbon-derived nanozymes, and other nanozymes have
433 been identified to possess OXD-like activity ⁷⁰⁻⁷³. The colorimetric biosensors can be developed
434 by utilizing the color change resulting from the catalytic process of oxidases, where the in situ
435 production of superoxide radicals and hydrogen peroxide oxidizes colorless substrates into colored
436 products ⁷⁴. To some extent, the OXD mimics are considered more appropriate for biochemical
437 analysis compared to the POD mimics due to their ability to function without the need for H₂O₂ in
438 the catalytic procedure. Additionally, the reaction situations for the enzyme mimics are simpler
439 and more direct. Nevertheless, Singh and colleagues determined that nanozymes possessing OXD-
440 like activity have the capability to trigger molecular oxygen conversion into reactive oxygen
441 species like singlet oxygen, oxygen radicals, and hydroxyl radicals during the catalytic mechanism,
442 which can be effectively utilized for the oxidation of diverse substrates⁷⁵⁻⁷⁷. This results in a lack

1
2
3
4
5
6
7
8
9
10
11
12
13
14
15
16
17
18
19
20
21
22
23
24
25
26
27
28
29
30
31
32
33
34
35
36
37
38
39
40
41
42
43
44
45
46
47
48
49
50
51
52
53
54
55
56
57
58
59
60

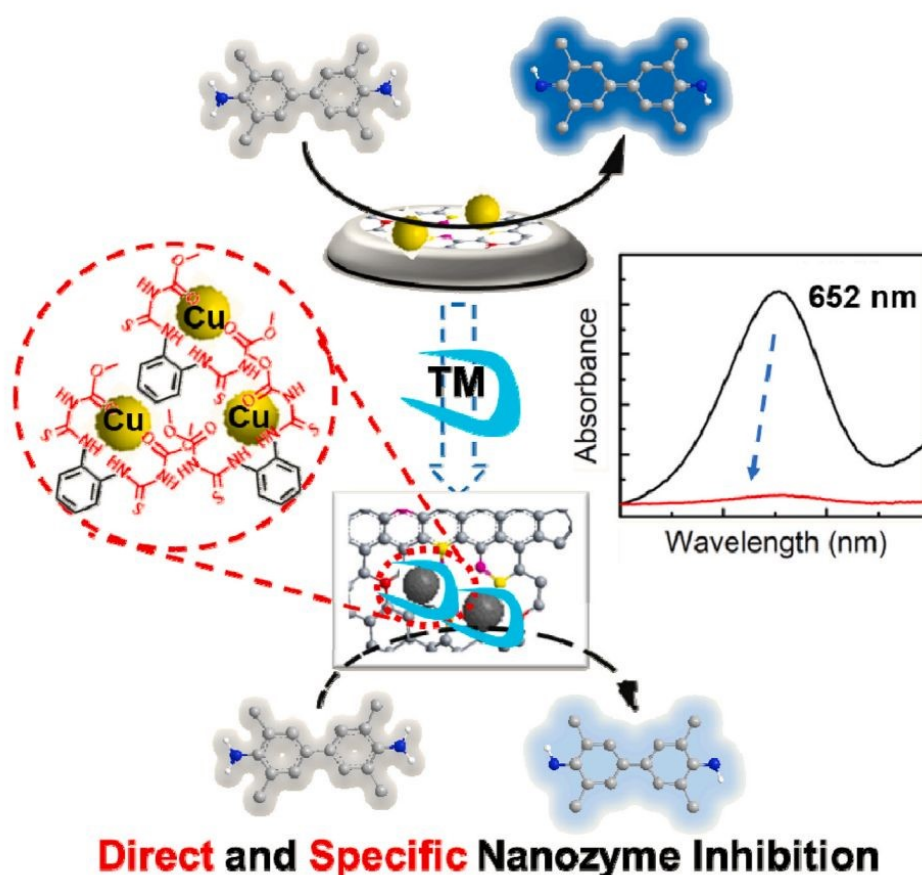
Open Access Article. Published on 20/04/2024. Downloaded on 20/04/2024 14:22:04.
This article is licensed under a Creative Commons Attribution-NonCommercial 3.0 Unported Licence.



1
2
3 443 of specificity in the catalytic activity of the nanozymes during the substrate process. In order to
4
5 444 address this issue, they developed a biomimetic approach utilizing MOF materials. Through the
6
7 445 manipulation of MOF crystal growth in the Z direction, researchers successfully synthesized
8
9 446 ultrathin nanosheets of Mn-UMOF using benzene dicarboxylic acid and triethylamine. The
10
11 447 presence of the robust donor ligand triethylamine and the bridging ligand benzene dicarboxylic
12
13 448 acid in Mn-UMOF leads to an increased density of active sites and enhanced substrate binding
14
15 449 properties, particularly for electron unsaturated, when compared to the bulk Mn-BMOF.
16
17 450 Additionally, Mn-UMOF could better catalyze the substrates oxidation like amplex red (AR),
18
19 451 ABTS, and TMB without the any external oxides addition ⁷⁸.
20
21 452 In another study, Zhang's team established an innovative technique that can selectively identify
22
23 453 thiophanate-methyl ⁷⁹. A Cu-doped carbon nanozyme, denoted as Cu@NC, was developed with
24
25 454 Cu serving as the active center site. The thiocarbamide-like and ethylenediamine-like buildings in
26
27 455 the target analyte, thiophanate-methyl exhibit a robust affinity for metal ions. This property enables
28
29 456 thiophanate-methyl to selectively interact with Cu@NC in the existence of other pesticides,
30
31 457 leading to a significant reduction in the catalytic performance of the nanozyme and facilitating
32
33 458 colorimetric detection (Figure 2). The researchers also examined the specificity of the colorimetric
34
35 459 sensor and revealed that thiophanate-methyl had a direct and specific inhibitory effect on the OXD
36
37 460 performance of Cu@NC nanozymes. To examine the mechanism through which the nanozymes
38
39 461 activity is inhibited, experiments were carried out. These experiments revealed a reduction in the
40
41 462 nanozymes catalytic activity after pre-incubating the target molecule, thiophanate-methyl, with
42
43 463 Cu@NC. Subsequently, the thiophanate-methyl was introduced to the chromogenic substrate.
44
45 464 Upon the introduction of thiophanate-methyl into the conventional system consisting of TMB and
46
47 465 Cu@NC, it was observed that the catalytic activity remained unaffected. This suggests that the
48
49
50
51
52
53
54
55
56
57
58
59
60

1
2
3 466 decrease in Cu@NC activity caused by thiophanate-methyl is a result of its direct interaction with
4
5 467 Cu@NC, rather than from enhancing the reduction of oxTMB. Additional inhibitory elements
6
7
8 468 were subsequently examined, and it was lastly found that TM can be fixed onto the Cu@NC
9
10 469 interface via π - π stacking interactions and attached to its metal sites to suppress its catalytic
11
12 470 function.
13

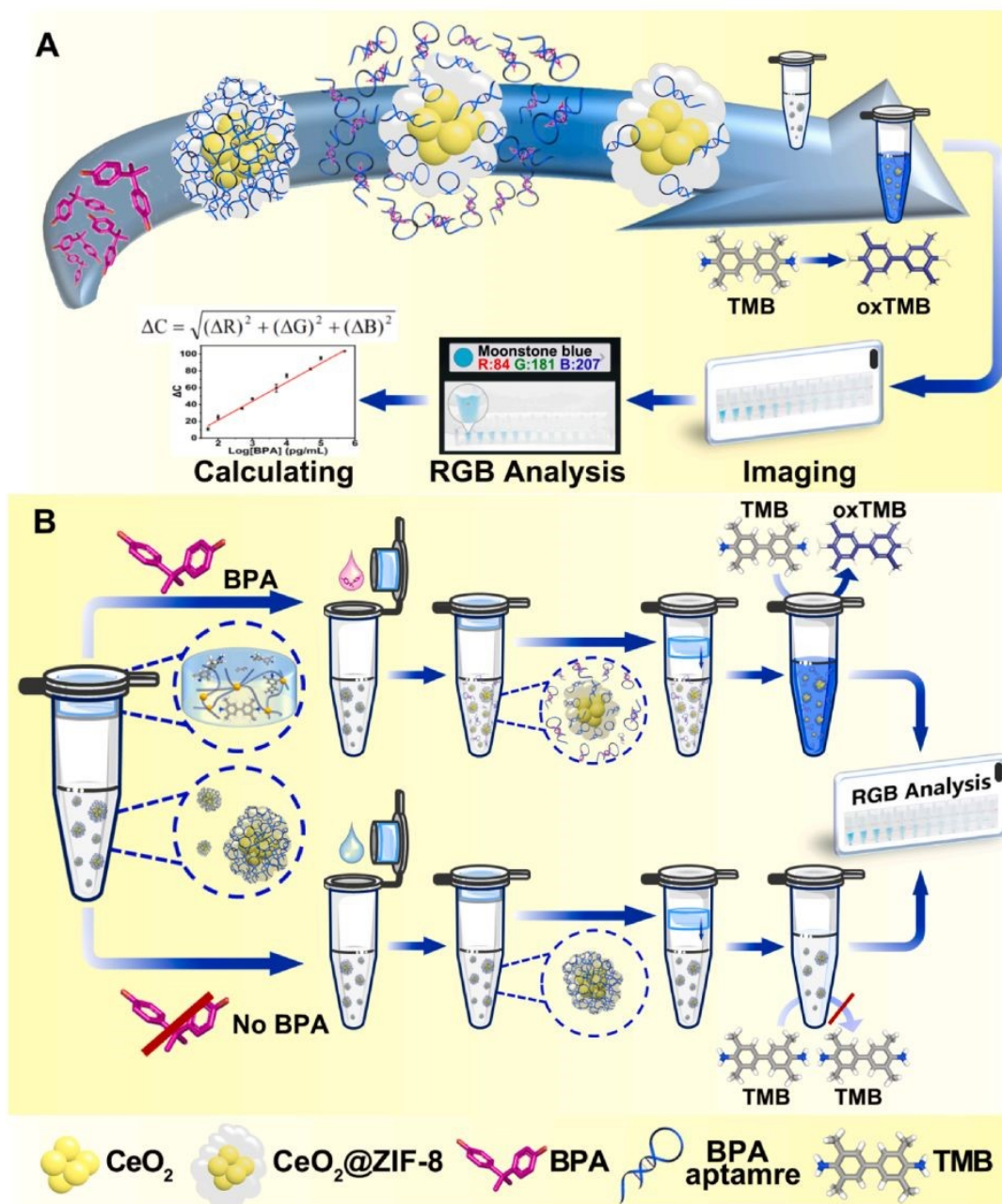
471



472

473 **Figure 2.** Diagram illustrating the development of a colorimetric nanoprobe utilizing the OXD-
474 like properties of nanozymes for the precise identification of thiophanate-methyl. Reprinted with
475 permission from Ref ⁷⁹.

1
2
3 476 CeO₂ nanoparticles demonstrate remarkable mimetic activity similar to oxidase enzymes, enabling
4
5 477 the catalysis of TMB color progress in the absence of hydrogen peroxide. In this regard, Jia's group
6
7 478 developed a multifunctional incorporated portable colorimetric detecting substrate for the
8
9 479 determination of bisphenol A⁸⁰. As depicted in Figure 3, the experimental configuration utilized
10
11 480 the CeO₂@ZIF-8/Apt nanoprobe both the signal generation unit and recognition component.
12
13 481 Sodium alginate hydrogel tubes were employed to contain the TMB and catalytic reaction buffer
14
15 482 as the reaction medium. The hydrogel containing the TMB platform was attached to the top of the
16
17 483 tube, while the signal probe was placed at the base of the tube. Following the introduction of the
18
19 484 sample and subsequent mixing with the signal probe, the Apt molecules on the signal probe
20
21 485 dissociated and attached to the target, which resulted in the triggering of the OXD activity from
22
23 486 the CeO₂@ZIF-8. Upon completion of the reaction process, photographs of the reaction solution
24
25 487 were taken using a smartphone subsequently uploaded to a color analysis based on the RGB app.
26
27 488 This method was employed to quantitatively evaluate the target object.
28
29
30
31
32
33
34
35
36
37
38
39
40
41
42
43
44
45
46
47
48
49
50
51
52
53
54
55
56
57
58
59
60



489

490 **Figure 3.** (A) Diagram description of the fabrication and the OXD-like properties of CeO₂@ZIF-

491 8/Apt nanoprobes. (B) The sensing mechanism of one-pot portable testing substrate for bisphenol

492 A determination. Reprinted with permission from Ref⁸⁰.

493 2.3. Catalase-like activity

494 The catalase enzyme facilitates the degradation of hydrogen peroxide into oxygen and water. The
495 catalase-like properties of NPs were first reported in amine-terminated PAMAM dendrimers that
496 encapsulated gold nanoclusters, which were observed in both physiological and acidic
497 conditions⁸¹. Likewise, several nanozymes-like manganese oxide (Mn₃O₄) nanoparticles, platinum
498 nanoparticles, and cerium oxide nanoparticles are defined to display the catalase-like activity. The
499 molecular-level investigation of the catalase-like behavior of nanozymes explores mechanisms
500 involving bi-hydrogen peroxide association, base-like dissociation, or acid-like dissociation⁸².
501 The bi-hydrogen peroxide mechanism has been identified as the most appropriate explanation for
502 the catalase-like activity in nanozymes, particularly in the case of cobalt (II, III) oxide (Co₃O₄)
503 nanoparticles. The catalase-like activity of cerium oxide nanoparticles involves the oxidation of
504 hydrogen peroxide on the nanoparticles' surface to form oxygen. This process leads to the
505 reduction of cerium oxide to H₂-ceric oxide. Subsequently, H₂-ceric oxide reacts with another
506 hydrogen peroxide molecule, resulting in the production of water⁸³. Further, Zhang et al. illustrated
507 the catalase-like function of iron-based single atom nanozymes (Fe-SANzymes) considered via
508 obviously exposed edge-hosted defective FeN₄ atomic sites⁸⁴. The mechanistic investigation
509 demonstrates that defects facilitate a substantial charge transfer from the Fe atom to the carbon
510 matrix. This process activates the central Fe atom, enhancing its interaction with hydrogen
511 peroxide and simultaneously weakening the O-O bond.

512 2.4. Multi-enzyme-like activity


513 Nanozymes with CAT-like function are frequently employed to eliminate extra naturally
514 happening reactive oxygen hydrogen peroxide, which is somewhat close to POD enzymes.
515 Nevertheless, nanozymes typically lack the capability to oxidize substrates to enable hue advance.

1
2
3 516 Consequently, it is less frequent to depend solely on the nanozymes in terms of the CAT activity
4
5 517 for the fabrication of colorimetric nanoprobe. Superoxide dismutase is a metalloenzyme with
6
7 518 antioxidant properties found in various organisms, capable of enabling the dismutation of reactive
8
9 519 superoxide anion radicals into O_2 and H_2O_2 . SOD enzymes like CAT enzymes were frequently
10
11 520 employed to neutralize surplus reactive oxygen classes, playing a pivotal role in body's oxidation
12
13 521 and antioxidant equilibrium. The catalytic mechanism of SOD enzymes primarily entails the
14
15 522 protonation of superoxide anion ($O_2^{\cdot -}$), which in turn protonated by water to produce OH^- and
16
17 523 HO_2^{\cdot} radicals. Nanozymes with $O_2^{\cdot -}$ scavenging capability are deliberated to be favorable
18
19 524 substitutes to natural SOD enzymes. If nanozymes demonstrate multiple simulated enzyme
20
21 525 functions simultaneously, like SOD, OXD, and POD, the dominant activity is expected to be the
22
23 526 SOD enzyme activity. This activity is influenced by factors like environmental pH, surface ions,
24
25 527 and nanomaterial structure⁸⁵. Currently, the majority of reported nanozyme activities focus on
26
27 528 POD and OXD activities, with limited research on mimicking SOD activity. Moreover, given that
28
29 529 the primary purpose of the SOD enzyme is to preserve redox equilibrium in cells and mitigate
30
31 530 oxidative stress, a significant portion of research endeavors focusing on nanozymes with SOD-
32
33 531 mimetic characteristics are primarily directed towards mitigating inflammation. In contrast, there
34
35 532 is a conspicuous lack of research investigating the employment of SOD nanozymes in colorimetric
36
37 533 recognizing methodologies. Like CAT enzymes, the utilization of SOD-like nanozymes in
38
39 534 colorimetric probes typically depends on the multifunctional enzyme properties of the nanozymes.

4. The application of nanozyme based on the colorimetric biosensor for biotoxins detection

50 536
51
52
53
54
55
56
57
58
59
60

Open Access Article. Published on 09/10/2024. Downloaded on 09/10/2024 14:22:04.
This article is licensed under a Creative Commons Attribution-NonCommercial 3.0 Unported Licence.



537 4.1. Mycotoxins detection

538 Mycotoxins, as one of the most alarming food and feed contaminants, are carcinogenic and highly
539 toxic secondary metabolites produced by specific fungi, predominantly molds, which have the
540 potential to contaminate a broad spectrum of crops (including nuts, grains, and legumes) and this,
541 in turn, can be transferred to various food products. These naturally occurring toxins pose a
542 substantial risk to both human, with exposure capable of inducing numerous adverse effects such
543 as acute poisoning, chronic ailments, and potentially cancerous consequences. Mycotoxins are
544 typically prevalent in cereals, grains, nuts, spices, coffee, cocoa, dried fruits, and animal-sourced
545 products such as milk and meat. Prominent and extensively researched mycotoxins comprise
546 aflatoxins, ochratoxins, fumonisins, trichothecenes, and zearalenone ^{86, 87}. Therefore, the
547 implementation of effective and innovate mycotoxin analytical detection methods, and alongside
548 that, novel nanomaterials has become pivotal for safeguarding humans against health dangers and
549 risks. This section has been conducted to review the major mycotoxins, including aflatoxin B₁
550 (AFB₁) and ochratoxin A (OTA), detection based on nanozymes.

551


552 4.1.1. Aflatoxin

553 Aflatoxins are hazardous secondary metabolites primarily synthesized by *Aspergillus fungi*. These
554 toxins reveal significant mutagenic, carcinogenic, and teratogenic potency in both human and
555 animal subjects. Corn, rice, peanuts, dried fruits, spices, and dairy products can be considered the
556 most important source of these toxins. Among different aflatoxins, AFB₁ introduced the most

perilous member of the aflatoxin group, as a group 1 carcinogen, responsible for major of all aflatoxins-associated feed and food contamination^{88, 89}. In this regard, the maximum allowable limits of AFB₁ in foodstuffs were set a 1.0–20 µg/kg. The field of biosensors based on various nanozymes including single-atomic nanozymes⁹⁰, MOFs⁵⁵, and metal nanoparticles¹⁹ is rapidly evolving, with ongoing research focused on understanding their mechanisms of action and increasing their catalytic efficiency. In favor of the application of metal nanoparticles as nanozymes, two metal components demonstrate better peroxidase catalytic performance than monometallic nanozymes. For example, Zhao et al.⁹¹, reported a surface-enhanced Raman scattering (SERS) sensor based on gold-mercury nanoparticles (Au@HgNPs) coupled with carbon dots (CDs) for AFB₁ determination. In this study, the poor colloidal stability and low enzyme-like activity of the AuNPs were distinctly improved by using Hg²⁺. This modification could be beneficial for the oxidase-mimicking activity of the AuNPs, attributing to Hg²⁺ reduced to the metallic (Hg⁰) forming Au@HgNPs. Under optimal conditions, the presence of the target inhibited the aggregation of Au@HgNPs particles, through oxygen atoms in the carbonyl group, which caused SERS intensity. In 2022, Lai et al.⁹², focused on introducing a simple and rapid synthesis method of nanozyme by simply mixing Cu(II) and K₃[Fe(CN)₆] for presenting a copper hexacyanoferrate nanoparticles (CHNPs) in terms of AFB₁ detection. Elaborately, in contrast to the common nanozyme synthesis methods which rely on re-synthesized nanomaterials, the nanozyme was designed in this biosensing platform without requiring the tedious process and preparation of nanomaterials. Therefore, this biosensing approach can broaden our horizon about another important factor in terms of the application nanozyme in detection, which is tedious nanozyme preparation, by offering a simple, rapid, and accessible way to generate the nanozyme on-demand. Interestingly, bimetal nanozymes demonstrate better catalytic efficacy compared to

1
2
3
4
5
6
7
8
9
10
11
12
13
14
15
16
17
18
19
20
21
22
23
24
25
26
27
28
29
30
31
32
33
34
35
36
37
38
39
40
41
42
43
44
45
46
47
48
49
50
51
52
53
54
55
56
57
58
59
60

Open Access Article. Published on 09/09/2024. Downloaded on 09/09/2024 14:22:04.
This article is licensed under a Creative Commons Attribution-NonCommercial 3.0 Unported Licence.



1
2
3 580 their single-metal counterparts, owing to the synergistic interplay between the two metal varieties.
4
5 581 Most recently, Wu and co-workers⁹³, exploited mesoporous SiO₂/gold-platinum (Au-Pt), m-SAP,
6
7 582 in the structure of colorimetric biosensing device for AFB₁ detection. In this protocol, the
8
9 583 mesoporous of SiO₂ nanospheres were loaded with Au-Pt, enjoying high catalase like activity. In
10
11 584 the absence of the target, the complementary DNA conjugated m-SAP was captured by aptamer-
12
13 585 magnetic nanoparticles and facilitated the 3,3',5,5'-tetramethylbenzidine (TMB)/H₂O₂ coloring
14
15 586 system. The detection limit of the developed colorimetric aptassay was 5 pg/mL, 600-fold lower
16
17 587 than that of traditional ELISA. In addition, during interference testing, AFB₁ could be
18
19 588 differentiated from six other interfering substances. In order to achieve more a reliable and highly
20
21 589 sensitive nanozyme based on two metal varieties, Jiang and colleagues⁹⁴, exploited the advantages
22
23 590 of bimetallic MoS₂/Au nanozyme, as a substrate for immobilization of aptamer, in developing of
24
25 591 sandwich-based colorimetric aptasensor of AFB₁ (Figure 4). In this work, the synergic effect
26
27 592 between MoS₂ and Au increased catalysis activity and stability. In detail, the low Michaelis
28
29 593 constant (K_m) and the high maximum reaction rate (V_{max}) of MoS₂/Au in comparison of single-
30
31 594 component MoS₂ or Au nanomaterials demonstrated that stronger binding affinity and superior
32
33 595 catalytic efficiency, respectively. Importantly, the specific structure, the flower-like MoS₂/Au
34
35 596 composite, introduced numerous surface-active sites through its unique multilayered and porous
36
37 597 structure which was considered an excellent immobilization substrate of aptamers. Furthermore,
38
39 598 the high surface area and porous structure of silica aerogel modified stainless-steel mesh
40
41 599 (SiO₂/SSM) could immobilization of the negatively charged aptamer₂. Under normal
42
43 600 circumstances, the construction of sandwich aptassay was conducted by capturing AFB₁ via
44
45 601 SiO₂/SSM, followed by binding of the MoS₂/Au/aptamer₁. This structure was successfully
46
47
48
49
50
51
52
53
54
55
56
57
58
59
60

employed to quantify AFB₁ in different real food samples including peanut, corn, and wheat, with negligible matrix effects (90.84%-106.11%) and recoveries of 88.52%-113.40%.

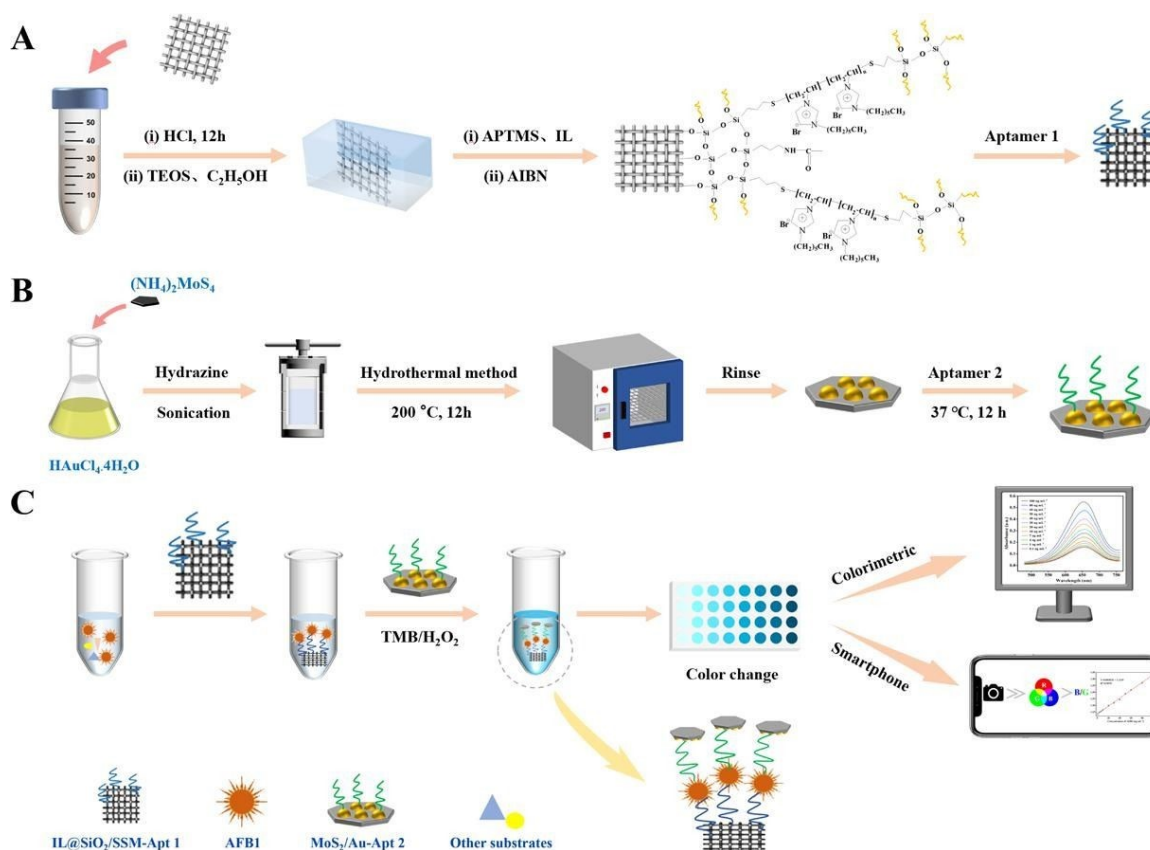
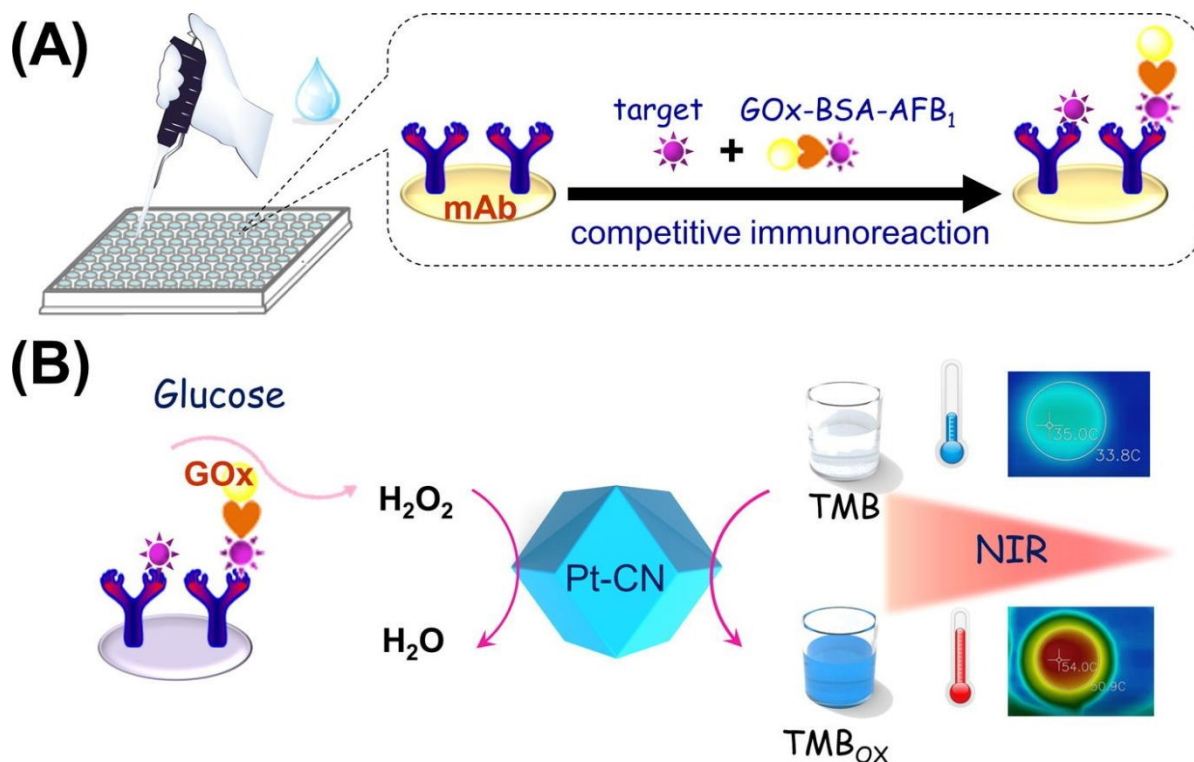


Figure 4(A-C). Representation of colorimetric aptasensor based on MoS₂/Au for AFB₁ determination. Reproduced with permission from ref⁹⁴ Copyright Elsevier Science, 2024.

Another excellent example of this concept was implemented in colorimetric and photothermal dual-mode immunoassay using peroxidase-like activity of Pt supported on nitrogen-doped carbon for AFB₁ quantification⁹⁵. As shown in Figure 5, the immune competition conducted between glucose oxidase (GOx)-labeled AFB₁-bovine serum albumin (BSA) and AFB₁, therefore releasing GOx to catalyze the glucose production of H₂O₂. Under normal condition, the colorimetric signal was produced due to oxidization of TMB to TMBOx. Along with the colorimetric signal, a thermal

613 signal was achieved when TMB_{OX} underwent photothermal conversion under 808 nm laser
614 irradiation. The fabricated biosensor was able to detect AFB₁ with a LOD of 0.22 and 0.76 pg/mL.



615
616 **Figure 5.** (A) Competitive-based immunosensor exploiting GOx-labeled AFB₁-BSA conjugate as
617 the tag. (B) Illustration colorimetric and photothermal measurement based on H₂O₂-responsive
618 peroxidase-like activity of Pt-CN. Reproduced with permission from ref ⁹⁵. Copyright Elsevier
619 Science, 2019.

620 The application of multimodal biosensors based on nanzyme in AFB₁ determination can
621 introduce different signals, extending the linear range of quantification. In addition, these signals
622 can verify each other to improve the accuracy of biosensing approaches ^{96, 97}. Another dual-mode
623 approach for AFB₁ quantification based on Ag@Au IP6 bifunctional nanzyme, with peroxidase-
624 like activity and SERS effect, was reported by Tan and colleagues ⁹⁸. For this purpose, the surface
625 of magnetic particles was decorated with AFB₁ aptamers along with a trigger probe. In the presence

1
2
3
4
5
6
7
8
9
10
11
12
13
14
15
16
17
18
19
20
21
22
23
24
25
26
27
28
29
30
31
32
33
34
35
36
37
38
39
40
41
42
43
44
45
46
47
48
49
50
51
52
53
54
55
56
57
58
59
60

of the target, the conjugation of targets with specific aptamers led to the trigger probe and this, in turn, initiated a hybridization chain reaction (HCR) which introduced alkaline phosphatase (ALP), catalyzing the self-assembly of the Ag@Au IP6 nanozyme. The constructed nanozyme revealed increased peroxidase-like activity, improving the oxidation of TMB to the blue-colored TMBOx, additionally, the core-shell structure of that also enabled strong SERS enhancement of the TMBOx signal.

Particularly, in light of economic discussion, substituting precious metals, which contribute to nanozymes, with more affordable transition metals, using in the structure of nanozymes can markedly diminish the expenditure associated with nanozymes. For instance, Cai et al.⁹⁹, designed a novel colorimetric nanozyme-based lateral flow assay (LFA) based on MnO₂ nanosheets (MnO₂ NSs) as an oxidase mimics and catalytic label for AFB₁ determination. As shown in Figure 6A, the test (T) line of the strip was decorated with anti-AFB₁ antibody-conjugated MnO₂ NSs for capturing AFB₁. Attractively, thanks to the properties of MnO₂ NSs in catalyzing the oxidation of TMB, TMB solution was added onto the T-line. When the target was added to the immunosensing device, the oxidation could provide a visual color signal which was inversely proportional to the AFB₁ concentration in the sample. The reported nanozyme-strip bioassay revealed a LOD of 15 pg/mL for AFB₁, over 100-fold lower than the maximum limit set by the European Union. On the other hand, both of the instability of the colloidal nature of nanozymes and their complicated interactions with bioreceptors can limit nanozyme exploitation in LFA. In this light, it is crucial to rationally design nanozyme-based signal labels with features that facilitate easy functionalization, good dispersibility, distinctly visible color, and enzymatic activity¹⁰⁰. These features are pivotal for increasing the applicability of nanozymes in LFA applications. A good example of this concept was prepared in another transition metal, CuCo, which was coated by polydopamine (PDA) with

1
2
3
4
5
6
7
8
9
10
11
12
13
14
15
16
17
18
19
20
21
22
23
24
25
26
27
28
29
30
31
32
33
34
35
36
37
38
39
40
41
42
43
44
45
46
47
48
49
50
51
52
53
54
55
56
57
58
59
60

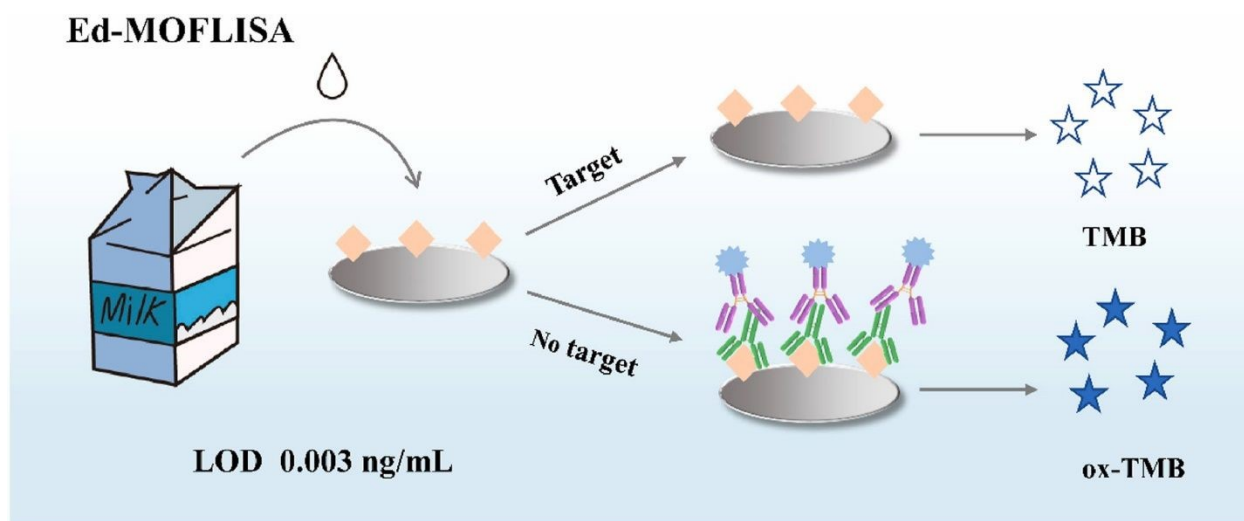
Open Access Article. Published on 20/04/2024. Downloaded on 20/04/2024 14:22:04.
This article is licensed under a Creative Commons Attribution-NonCommercial 3.0 Unported Licence.



1
2
3 649 excellent biocompatibility, good adhesion, and rich functional groups (chinone, imine, and amine),
4
5 650 leading to good hydrophilicity and binding ability with biomolecules ¹⁰¹. In this protocol, the
6
7 651 carboxyl-functionalized aptamers were conjugated with CuCo@PDA nanozyme via amide
8
9 652 condensation reactions. The fabricated probe was used on the surface of the T line and the
10
11 653 difference of color with/without the presence of the target was the principle of detection (Figure
12
13 654 6B). Further, the ability of the nanozyme to catalyze the oxidation of TMB-H₂O₂ could amplify
14
15 655 the color change on the T-line. To illustrate, the visual LOD was reduced to 0.1 ng/mL by the
16
17 656 TMB-H₂O₂ catalytic amplification. In 2024, Fan and colleagues ¹⁰², designed another
18
19 657 functionalized nanozyme, flower-like L-cysteine-functionalized FeNi bimetallic nanoparticles (L-
20
21 658 Cys-FeNiNPs), with excellent peroxidase-like catalytic activity in colorimetric aptasensor for
22
23 659 detection of AFB₁. In the reported nanozyme, the peroxidase-like activity was attributed to the
24
25 660 generation of superoxide radicals ($\bullet\text{O}_2^-$) and holes (h^+) that were produced through the catalysis,
26
27 661 and alongside that, the high selectivity of probe was described as the conjugation of specific
28
29 662 aptamer with L-Cys-FeNiNPs via EDC/NHS chemistry and streptavidin-biotin interaction. Indeed,
30
31 663 like previous modification, the decoration of FeNiNPs with L-Cys not only can help increase the
32
33 664 dispersibility and stability of the FeNiNPs, but also the biocompatibility and functionalization
34
35 665 capability of nanozyme significantly improved. In the presence of the target, the reduction of the
36
37 666 active sites of the L-Cys-FeNiNPs suppressed the TMB oxidation and reduced the color signal.
38
39
40
41
42
43
44
45
46
47
48
49
50
51
52
53
54
55
56
57
58
59
60

1
2
3 674 porphyrin (PCN)-based organic linkers were employed for self-assembly with metal nodes,
4
5 675 leading in the development of MOFs with different structures and functions. On the other hand,
6
7 676 accessing the active sites within MOFs remains challenging. One of the efficient solutions is based
8
9 677 on hybrid nanomaterials, which have been attributed to using platinum nanoparticles Pt NPs on
10
11 678 two-dimensional support substrates ^{103, 104}. As example, Zhang et al. ¹⁰⁵, reported a novel
12
13 679 colorimetric approach exploiting Pt@PCN-222 nanozyme, with oxygen vacancies, for AFB₁
14
15 680 detection. The detection principle of this study was operated according to the oxidization of the
16
17 681 2,2'-azino-bis(3-ethylbenzthiazoline-6-sulfonic acid (ABTS) substrate to produce a blue-green
18
19 682 colored product. In the presence of the target, the binding of Pt@PCN-222 with the target caused
20
21 683 inhibition which decreased the number of active Pt@PCN-222 conjugates available for the ABTS
22
23 684 oxidation reaction. Another technique for addressing accessibility to the active sites of MOFs is
24
25 685 operated based on a synthesis technique, NanoMOFs, can accelerate substrate diffusion in catalytic
26
27 686 MOF material and this, in turn, provides greater external surface area and lower diffusion barriers.
28
29 687 For instance, Peng and co-workers ¹⁰⁶, developed a sensitive, reproducible, and accurate
30
31 688 colorimetric immunoassay based on NanoPCN-223(Fe) with high peroxidase-like activity and
32
33 689 excellent dispersion for AFB₁ determination (Figure 7). In detail, the implantation of NanoPCN-
34
35 690 223(Fe) in the structure of colorimetric technique which produced color by catalyzing the
36
37 691 oxidation of the colorless substrate TMB in the presence of H₂O₂. To illustrate, through the
38
39 692 catalyzing process, the nanozyme generated hydroxyl radicals (\bullet OH), from H₂O₂, which oxidize
40
41 693 the TMB substrate, converting the colorless TMB to the blue ox-TMB. Under normal conditions,
42
43 694 the conjugation of the nanozyme and the target inhibited catalyzed oxidation of TMB which
44
45 695 reduced the intensity of color.
46
47
48
49
50
51
52
53
54
55
56
57
58
59
60

696 All things considered, the application of nanozymes based on metal nanoparticles and MOFs can
697 be considered efficient materials for aflatoxins detection. The investigation of these materials is
698 based on two metals varieties, bimetallic and affordable materials, and alongside that, the
699 amplification techniques can broaden our horizon about the performance of nanozymes in
700 colorimetric approaches for the detection of aflatoxins.

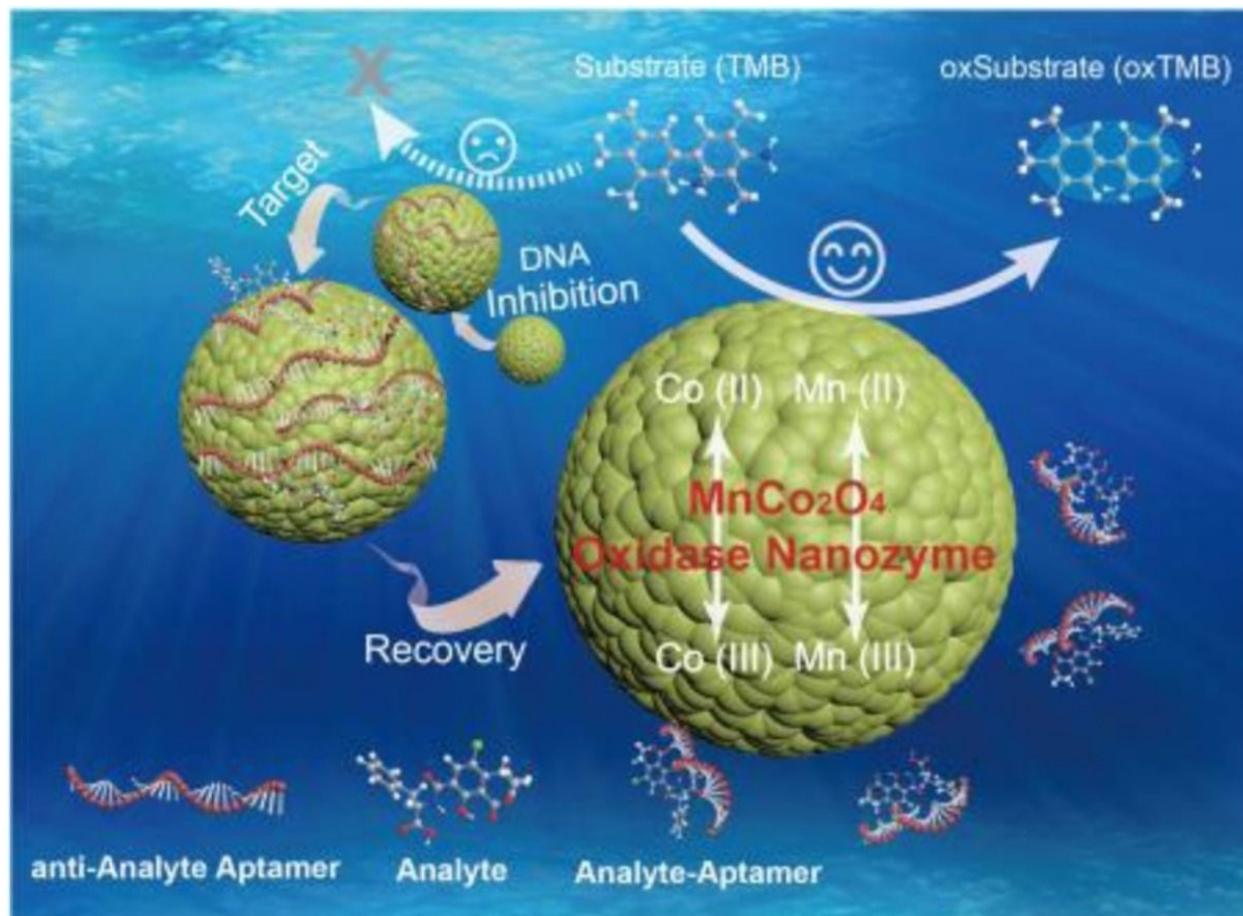


701
702 **Figure 7.** Illustration of the application of NanoMOFs for colorimetric detection of AFB₁.
703 Reproduced with permission from ref¹⁰⁶. Copyright Elsevier Science, 2022.

704 4.1.2. Ochratoxin A

705 According to the International Agency for Research on Cancer, Ochratoxin A, as a possibly
706 carcinogenic to humans (Group 2B), is classified as one of the significant mycotoxins. To
707 elaborate, high chemical stability against heat treatments and hydrolysis through food processing
708 makes it one of the most dangerous poisons for human. This mycotoxin originates from the species
709 of fungi including *Penicillium verrucosum*, *Aspergillus carbonarius*, *Aspergillus ochraceus*, and
710 *Aspergillus niger*^{107, 108}. Over the last decades, the advent of nanozyme has revolutionized multiple
711 domains in detection of OTA. Interestingly, the investigation of common structures of reported

712 nanozymes can open new doors in terms of quantification of OTA. One of the common structures
 713 is spinels which form huge families, and they consist of one or more metal elements. Among them,
 714 spinel-type metal oxides, with the formula of AB_2O_4 , enjoy superior promoting nanozyme
 715 performance over other metal oxides due to controllable structure, composition, valence, and
 716 morphology^{109, 110}. For example, Huang and co-workers¹¹¹, employed OTA-specific aptamer on
 717 the surface of manganese cation substituted cobalt oxide ($MnCo_2O_4$) for OTA determination. As
 718 shown in Figure 8, the attachment of aptamer on the surface of the nanozyme inhibited the
 719 nanozyme activity of spinel $MnCo_2O_4$ through aptamer-target complex, presenting a new
 720 colorimetric aptasensor. Under normal conditions, the developed aptasensor could able to detect
 721 OTA with a LOD of 0.08 ng/mL.



722

 1
2
3
4
5
6
7
8
9
10
11
12
13
14
15
16
17
18
19
20
21
22
23
24
25
26
27
28
29
30
31
32
33
34
35
36
37
38
39
40
41
42
43
44
45
46
47
48
49
50
51
52
53
54
55
56
57
58
59
60


723 **Figure 8.** Schematic of using MnCo_2O_4 in the structure of colorimetric aptasensor for OTA
724 determination. Reproduced with permission from ref ¹¹¹. Copyright Elsevier Science, 2018.

725 The distribution of cations among the octahedral and tetrahedral sites in the crystal structure can
726 introduce inverse spinel structure, with a formula of $B(AB)O_4$, which demonstrates different
727 electronic and magnetic features compared to the spinel structure ¹¹². Most recently, Liu and
728 colleagues ¹¹³, improved the performance of anti-spinel structure by using Au and Pt in the
729 structure of Fe_3O_4 , through the ionic liquid (IL) as the cross-linker, for capturing synergistic
730 interaction between the alloy atoms. In this work, the surface of designed nanozyme was modified
731 with complementary DNA for conjugating with stainless steel mesh-aptamer. In the presence of
732 the OTA, the binding of the target with aptamer caused to separate signaling probe
733 ($\text{AuPt@IL@Fe}_3\text{O}_4$) and this, in turn, was used in a tube containing a tube with H_2O_2 and TMB for
734 observe the color change. All in all, the inverse spinel and spinel structures introduce the effective
735 bioreceptor immobilization and high catalytic activity, increasing the performance of biosensors.
736 However, the limited surface area and non-optimal electronic properties of spinel structure can
737 restrict their application. In terms of inverse spinel, although magnetic features and high catalytic
738 activity improve their performance, a complex synthesis processes can limit their nanozyme-based
739 application.

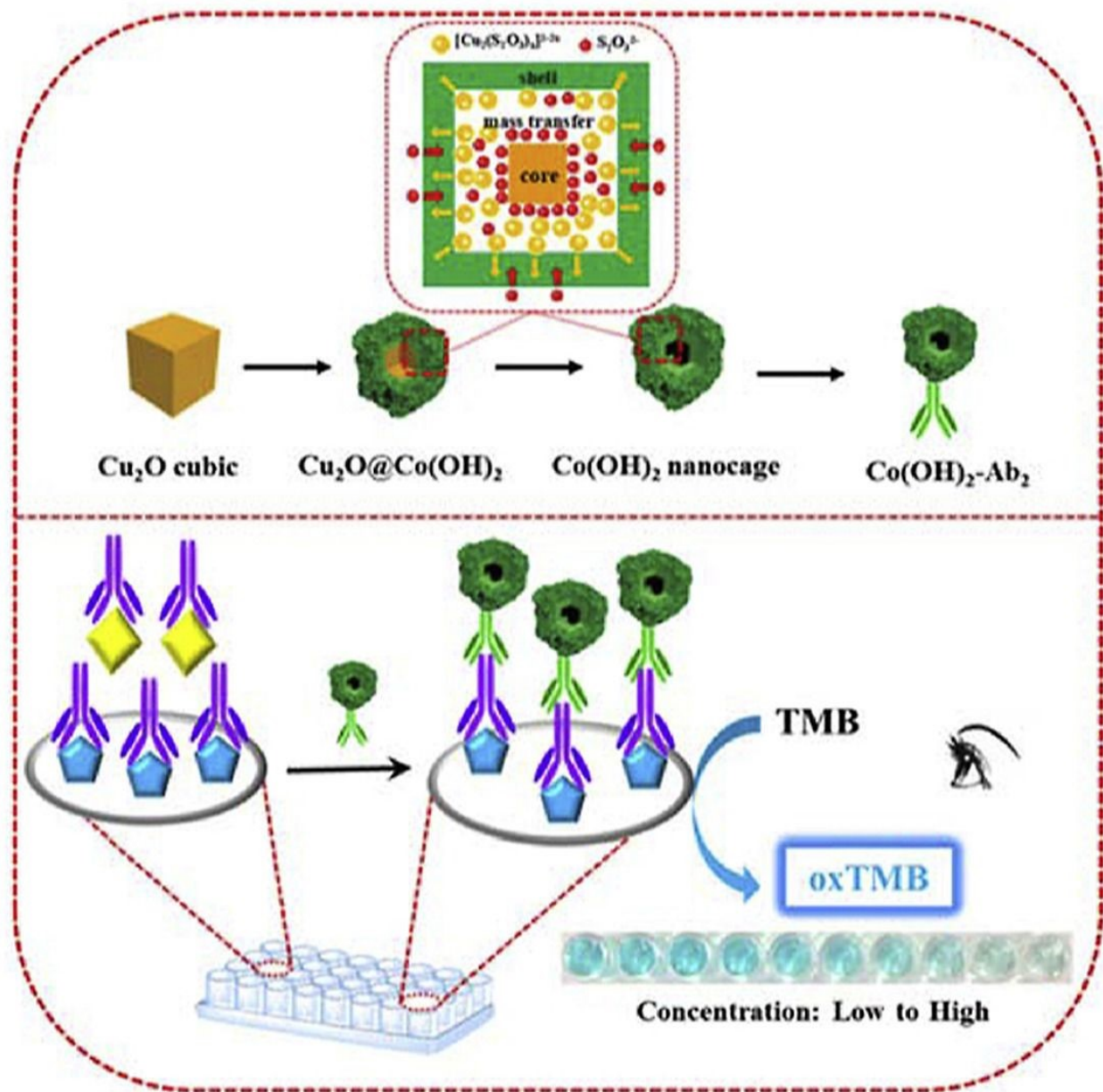
740 Along with these structures, tetragonal crystals and nanocubes structures are other structures used
741 in the development of nanozyme for OTA detection. To illustrate, tetragonal crystal systems have
742 been widely exploited in biosensors based on nanozyme owing to several advantages such as high
743 surface area to volume ratio, stability, electronic features, high catalytic activity, and versatile
744 functionalization ¹¹⁴. Currently, one of the excellent examples of using nanozyme-based tetragonal
745 crystal system for detection of OTA was developed by Tian and co-workers ¹¹⁵. In this protocol,

1
2
3
4
5
6
7
8
9
10
11
12
13
14
15
16
17
18
19
20
21
22
23
24
25
26
27
28
29
30
31
32
33
34
35
36
37
38
39
40
41
42
43
44
45
46
47
48
49
50
51
52
53
54
55
56
57
58
59
60

Open Access Article. Published on 09/04/2024. Downloaded on 2/22/2024 11:47:22 AM. This article is licensed under a Creative Commons Attribution-NonCommercial 3.0 Unported Licence.



1
2
3 746 the principle of this study was measuring the oxidase-mimicking activity of MnO₂ nanosheets. For
4
5 747 this purpose, the decoration specific aptamer on the surface of aptamer was exploited for capturing
6
7 748 OTA, leading to the production of the alkaline phosphatase-modified complementary DNA and
8
9 749 the cascade reaction is triggered by the product (ascorbic acid) of alkaline phosphatase catalysis.
10
11 750 The ascorbic acid reduced the oxidase-mimicking activity of MnO₂ nanosheets, leading to a pale
12
13 751 color of the enzyme catalytic substrate. Another structure is layer structure, with unique benefits,
14
15 752 which can provide efficient nanozymes in quantification of OTA. In 2020, Zhu et al. ¹¹⁶, fabricated
16
17 753 a novel colorimetric immunosensor based on cobalt hydroxide nanoparticle (Cu₂O) nanocubes,
18
19 754 with specific properties such as high surface area and high catalytic activity, for OTA
20
21 755 quantification (Figure 9). In detail, the decoration microwell plate with dopamine was modified
22
23 756 with OTA and ab₁ and, followed, Co(OH)₂-Ab₂ bounded to the prepared substrate. Under optimal
24
25 757 circumstances, the difference of the color changes of TMB from Co(OH)₂ nanocage in the absence
26
27 758 of H₂O₂ could present an efficient biosensing platform with a linear range and detection limit of
28
29 759 0.5 ng/L to 5 µg/L and 0.26 ng/L, respectively. Despite the high surface area and catalytic activity
30
31 760 of nanocubes structure, the stability issue in some conditions and aggregation of cubes be
32
33 761 considered important disadvantages of this structure. In addition, tetragonal crystal systems suffer
34
35 762 from limited surface area.
36
37
38
39
40
41
42
43
44
45
46
47
48
49
50
51
52
53
54
55
56
57
58
59
60



763

764 **Figure 9.** Illustration of colorimetric immunoassay based on Cu_2O nanocubes for detection of
 765 OTA. Reproduced with permission from ref¹¹⁶. Copyright Elsevier Science, 2020.

766 4.2. Marine toxins detection

767 Marine toxins, as poisonous substances, can be considered as natural metabolites which are
 768 produced by numerous such as bacteria, algae, and many marine invertebrates. Among them, algal
 769 toxins (including ciguatera toxin, domoic acid, and saxitoxin), invertebrate toxins, and some

 1
2
3
4
5
6
7
8
9
10
11
12
13
14
15
16
17
18
19
20
21
22
23
24
25
26
27
28
29
30
31
32
33
34
35
36
37
38
39
40
41
42
43
44
45
46
47
48
49
50
51
52
53
54
55
56
57
58
59
60

1
2
3 770 bacterial toxins may concentrate on various organisms through the food web. The negative
4
5 771 consequences of these toxins in both humans and animals are undeniable ^{117, 118}. Importantly,
6
7 772 various bioreceptors/receptors can improve the performance of nanozyme-based colorimetric
8
9 773 biosensors for determination of marine toxins. Antibodies, as one of the important bioreceptors,
10
11 774 have been used in antibody-antigen interaction for presenting sensitivity and specificity detection
12
13 775 approaches of marine toxins. Interestingly, the integration of nanozyme in the structure of
14
15 776 colorimetric immunosensors can improve analytical signal owing to the catalyzation of enzymatic
16
17 777 reaction by nanozyme, which increases the color intensity. For example, Hendrickson and co-
18
19 778 workers ¹¹⁹, conjugated Au@Pt nanozyme with an antibody for enhancing label of okadaic acid
20
21 779 quantification. The tendency of Au@Pt nanozyme to conjugate with anti-mouse antibodies, rather
22
23 780 than anti-okadaic acid antibodies, could provide an excellent situation for an indirect competitive
24
25 781 immunoassay format. This phenomenon led to unproductive immune binding without signal
26
27 782 change is excluded, resulting in improving sensitivity of immunoassay. When the target was added
28
29 783 to the system, the okadaic acid competed with the okadaic acid on conjugate pad for binding with
30
31 784 anti-okadaic acid antibodies and were immobilized on the T line of LFA.

32
33 785 The lack of chemical and thermal stability of antibodies, in harsh environmental circumnutates,
34
35 786 can make them sensitive to degradation and denaturation. Furthermore, the high cost of production
36
37 787 and purification of these bioreceptors can be considered another significant issue. In this regard,
38
39 788 competitive colorimetric was implanted in aptasensors based on AuNPs nanozyme for sensitive
40
41 789 and selective quantification of saxitoxin ¹²⁰. In this study, the competition of saxitoxin in samples
42
43 790 with immobilization saxitoxin was a principle of the developed aptassay. To illustrate, in the
44
45 791 presence of the target, the separation of specific aptamer from magnetic particles was conducted
46
47 792 and this, in turn, led to triggering the hybridization chain reaction. The colorimetric signal was
48
49
50
51
52
53
54
55
56
57
58
59
60

improved by amplifying catalytic activity of the AuNPs nanozymes. Similarly, in many colorimetric aptasensor studies, the adsorption of aptamer could promote the enzyme-like activity of AuNPs for saxitoxin determination^{121, 122}. Elaborately, this phenomenon could enhance surface negativity of nanozymes which increased adsorption and diffusion of positively charged substrates of TMB, improving of catalytic efficiency. In 2022, Li and colleagues¹²³, reported a novel aptasensor exploiting AuNPs@Fe²⁺ for multiple diarrheic shellfish poisons detection (Figure 10). Indeed, the performance of nanozyme, in terms of chemical stability and peroxidase-like activity, was improved by using Fe²⁺ in the structure of AuNPs. Furthermore, the high affinity of terminal-fixed aptamer (TF-DSP) was used in this study for the simultaneous detection of three diarrheic shellfish poisons. Under normal circumstances, the catalyze of TMB/H₂O₂/acetic acid due to the excellent peroxidase-like activity and the brilliant selectivity of aptamer could introduce a biosensing platform with a linear range and LOD of 0.4688–7.5 nM and 86.28 pM, respectively.

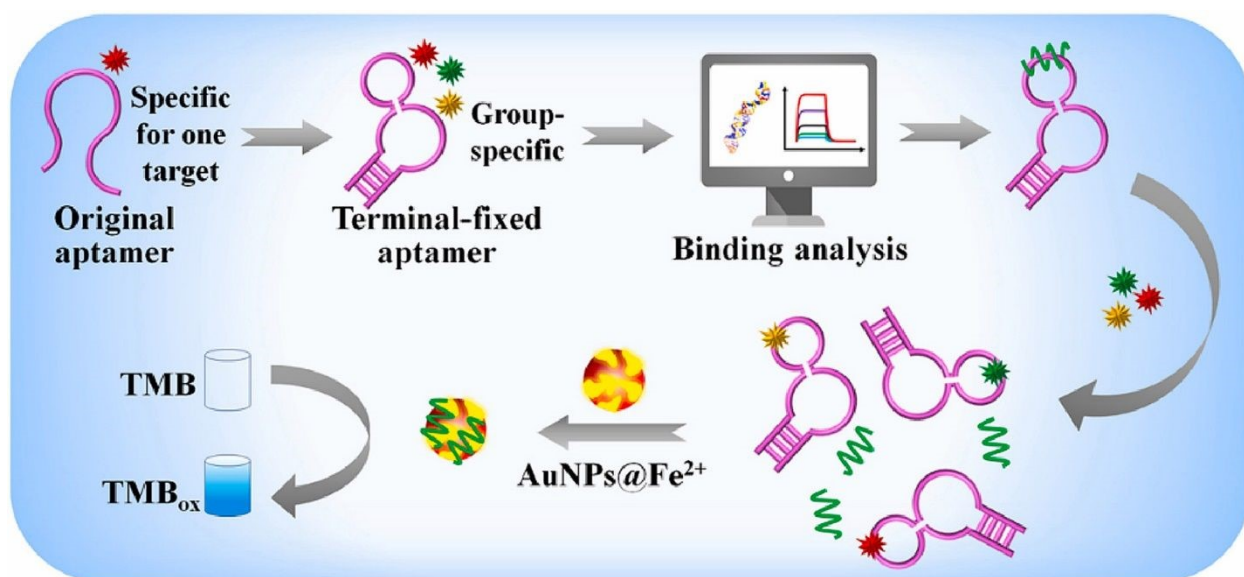


Figure 10. Schematic of colorimetric aptassay using decoration AuNPs with Fe²⁺ for multiple diarrheic shellfish poisons detection. Reproduced with permission from ref¹²³. Copyright Elsevier Science, 2022.


1
2
3 809 The complex immobilization process on the surface of nanozyme and the side effect of potential
4
5 810 interferences, in real samples, can considered the most important limitation of using aptamers in
6
7 811 the nanozyme structure. In addition, in terms of overcoming stability issues of combination of
8
9 812 antibodies with nanozyme, molecularly imprinted polymer (MIP), as artificial antibody and
10
11 813 antigen systems, attracted considerable attention for marine toxins detection ^{124, 125}. Most recently,
12
13 814 Wu et al. ¹²⁶, integrated a MIP with Au-Pt nanoparticles modified Fe₃O₄ magnetic nanozymes for
14
15 815 introducing an efficient biosensor of saxitoxin. For this purpose, Au-Pt nanoparticles were loaded
16
17 816 in Fe₃O₄ magnetic and, subsequently, thanks to the hydrolysis polymerization reaction, the
18
19 817 decoration modified Fe₃O₄ magnetic nanozymes with MIPs were prepared. In the presence of the
20
21 818 target, catalyzed the oxidation of TMB enabled the developed biosensing approach for detection
22
23 819 saxitoxin with a detection limit of 3.1 nM. Potential interference in signal transduction, durability,
24
25 820 and stability issues can be supposed most important limitation of MIPs. In order to address these
26
27 821 limitations, scholars must pay special attention to the fabrication optimized and compatible MIP-
28
29 822 nanozyme platforms. For instance, Cho and colleagues ¹²⁷, used peptide (as both the imprinting
30
31 823 template and the signal peptide), instead of antigen or aptamer, for designing competitive
32
33 824 colorimetric quantification of saxitoxin. In this light, the exploitation of specific peptides of
34
35 825 saxitoxin could overcome difficulty of aptamers and antibodies removal in biosensors based on
36
37 826 MIP-nanozyme. In addition, the integration MIP with specific peptide of saxitoxin was measured
38
39 827 with AuNP/Co₃O₄@Mg/Al. In the presence of the target, the less specific peptide of saxitoxin was
40
41 828 conjugated with MIP, leading to intensity of color change.

4.3. Bacterial food toxins

42 830 Nowadays, bacteria food toxin, which is macromolecule mainly of protein origin, is one the main
43
44 831 issues in the realm of food safety. These microorganisms can produce toxins in food or once the


1
2
3
4
5
6
7
8
9
10
11
12
13
14
15
16
17
18
19
20
21
22
23
24
25
26
27
28
29
30
31
32
33
34
35
36
37
38
39
40
41
42
43
44
45
46
47
48
49
50
51
52
53
54
55
56
57
58
59
60

Open Access Article. Published on 09/10/2024. Downloaded on 09/10/2024. This article is licensed under a Creative Commons Attribution-NonCommercial 3.0 Unported Licence.



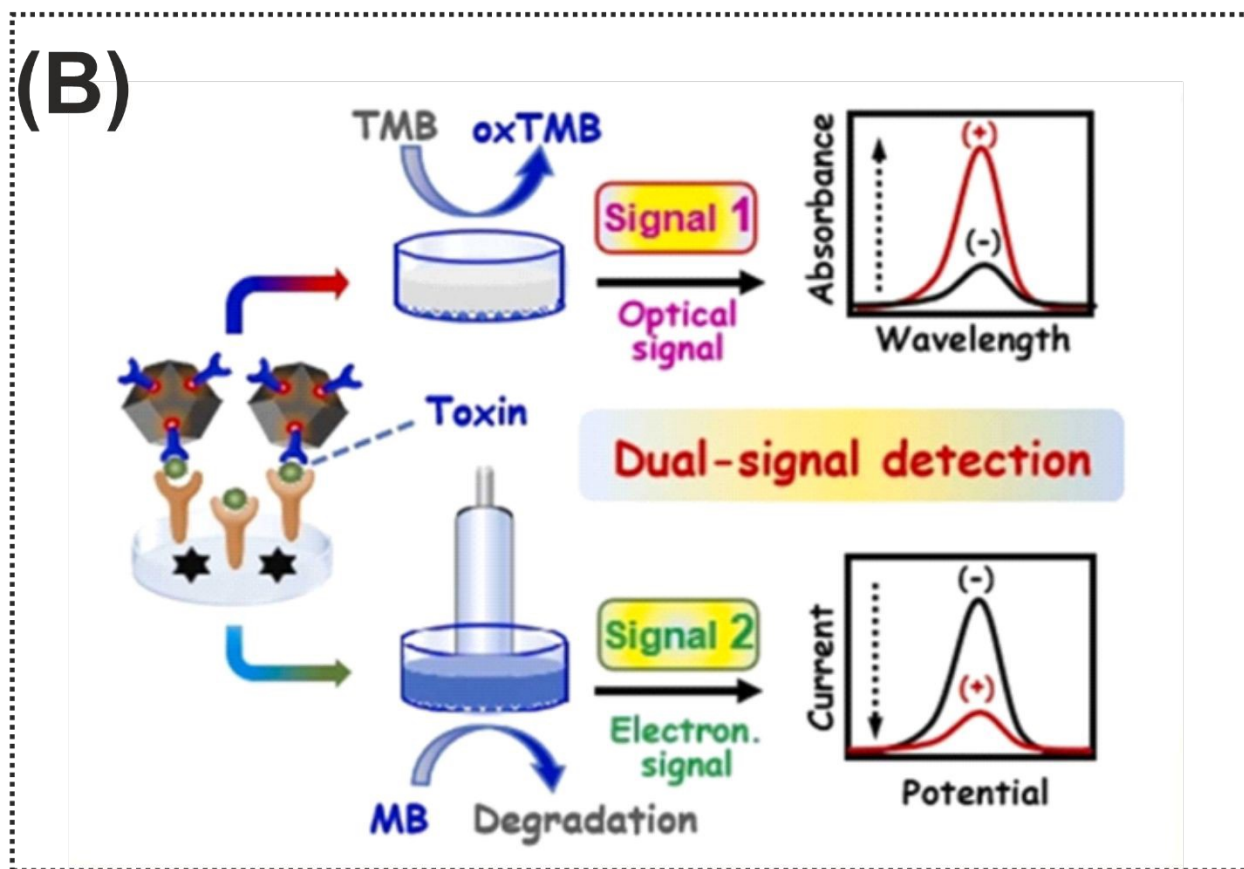
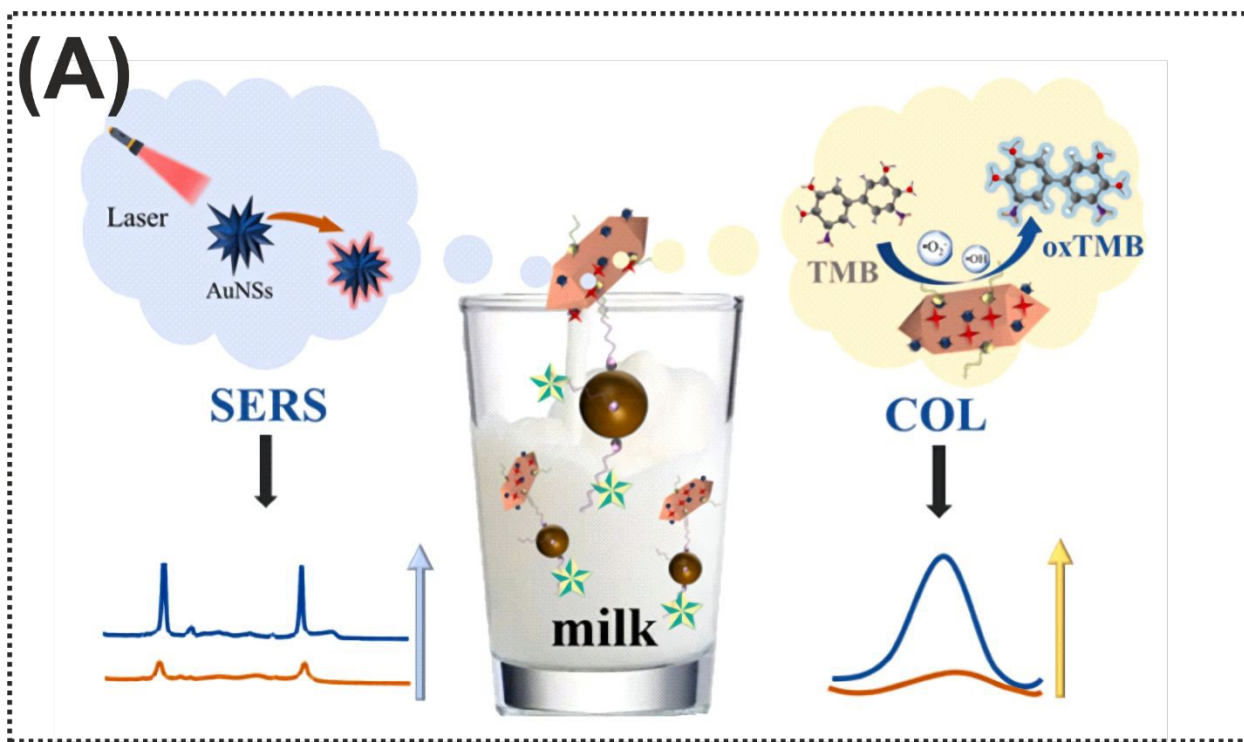
1
2
3 832 pathogen has colonized the digestive tract. These types of toxins damage in a specific organ of the
4
5 833 host. To illustrate, such toxins cause foodborne diseases including vomiting, nausea, abdominal
6
7 834 cramps, and diarrhea.^{128, 129}. Despite the fact that the field of research about detection bacterial
8
9 835 toxins is very wide, researchers attempted to use different nanomaterials in the structure of
10
11 836 nanozymes for amplification of detection signal. Various forms of Au-based nanomaterials such
12
13 837 as AuNPs gold nanostars (AuNSs) have been exploited as one of the important nanomaterials to
14
15 838 amplify the signal due to several benefits such as excellent stability, repeatability, and accuracy.
16
17 839 These nanomaterials gained great attention due to their ability to couple and integrate with different
18
19 840 bioreceptors and nanomaterials for acting as a nanozyme through chemical bonds and electrostatic
20
21 841 adsorption. As for labelling nanomaterials, Ren et al.¹³⁰, used the seed growth method for
22
23 842 assembling AuNSs in the structure of Mn/Fe-MIL(53) for introducing an efficient nanozyme in
24
25 843 colorimetric and SERS detection of Shiga toxin type II. As shown in Figure 11A, in terms of
26
27 844 construction signal probe which could oxidize colorless TMB into blue color oxTMB, the surface
28
29 845 of Mn/Fe-MIL(53) was decorated with AuNSs for providing an excellent for immobilization of
30
31 846 SH-complementary DNA, through Au-S bonding. In addition, in favor of capturing probe,
32
33 847 streptavidin-labeled magnetic beads were modified with a specific biotin-labeled aptamer. In the
34
35 848 presence of the target, the conjugation of aptamer with target the release of signal probes from the
36
37 849 complex and bring an enhancement of SERS and colorimetric signals. In the reported dual-mode,
38
39 850 the integration of SERS and colorimetric approaches introduced complementary and validated
40
41 851 results, improving the reliability of the Shiga toxin type II detection. In another example of Au-
42
43 852 based nanozymes, Liang and co-workers¹³¹, designed a novel dual-signal probe (AuPt
44
45 853 nanoparticle-loaded single atom nanocomposite, AuPt@Fe-N-C) for *Staphylococcus aureus*
46
47 854 enterotoxin B quantification (Figure 11B). For this purpose, the ab₁ was immobilized on the
48
49
50
51
52
53
54
55
56
57
58
59
60

Open Access Article. Published on 20/09/2024. Downloaded from https://pubs.rsc.org on 09/10/2024 14:22:04. This article is licensed under a Creative Commons Attribution-NonCommercial 3.0 Unported Licence.



1
2
3 855 surface of AuPt@Fe-N-C and this was used for sandwich structure. In addition to the target to the
4
5 856 system, the ab₁-*Staphylococcus aureus* enterotoxin B-ab₂ was performed in a 96-well plate which
6
7 857 could oxidate TMB from colorless to blue with a detection limit of 0.066 7 pg/mL. Along with
8
9 858 Au-based nanozyme, the unique properties and structure of rhodium (Rh), a non-toxic transition
10
11 859 metal, was exploited for staphylococcal enterotoxin B determination in milk samples ¹³². The
12
13 860 implementation of Rh, with peroxidase-like catalytic activity, on the sensing zone of LFA could
14
15 861 able to detect staphylococcal enterotoxin B with a detection limit of as low as 1.2 pg/mL.
16
17
18
19
20
21
22
23
24
25
26
27
28
29
30
31
32
33
34
35
36
37
38
39
40
41
42
43
44
45
46
47
48
49
50
51
52
53
54
55
56
57
58
59
60





862

1
2
3
4
5
6
7
8
9
10
11
12
13
14
15
16
17
18
19
20
21
22
23
24
25
26
27
28
29
30
31
32
33
34
35
36
37
38
39
40
41
42
43
44
45
46
47
48
49
50
51
52
53
54
55
56
57
58
59
60

1
2
3 863 **Figure 11. (A)** Representation of dual-mode colorimetric and SERS biosensor based on Mn/Fe-
4 MIL(53)@AuNSs for Shiga toxin type II detection. Reproduced with permission from ref ¹³⁰ (B)
5 864
6 865 Illustration of dual-signal electrochemical and colorimetric detection of *Staphylococcus aureus*
7 866 enterotoxin B ¹³¹. Copyright Elsevier Science, 2024.

867 **5. Theranostic applications of nanozymes for biotoxins**

868 Nanozymes catalytic theranostics introduces an innovative and novel strategy for theranostic
869 platforms, integrating detection and treatment in a single system ¹³³. The importance of these
870 platforms is highlighted in preventing the spread of biotoxins in contamination outbreaks by
871 intervention to neutralize biotoxins and monitoring them ¹³⁴. In favor of the detection of biotoxins,
872 catalytic color changing reaction conducts for achieving sensitive colorimetric sensors. In terms
873 of naturalization and degradation of biotoxins, the oxidation and hydrolysis of biotoxins break
874 these toxins by-products chemical down into non-toxic components by using nanozymes is an
875 efficient strategy for rendering them harmless ^{135, 136}. Numerous techniques were exploited for
876 biotoxins degradation such as UV method for marine biotoxins, demonstrating resistance to
877 photodegradation, On the other hand, high performance degradation with UV/S₂O₈²⁻ and
878 UV/H₂O₂ was achieved ^{137, 138}. In addition, biodegrading ATX-a into a nontoxic byproduct by
879 *Bacillus* strains such as *Bacillus flexus* SSZ01 and *Bacillus* strain AMRI-03 can supposed high
880 performance method for water treatment like rapid degradation of saxitoxins, which is directly and
881 indirectly associated with food safety ¹³⁹. Furthermore, MOF-derived nanozymes was used as a
882 high potential materials in the neutralization process ¹⁴⁰. Future research should be focused on the
883 theranostic application of nanozymes for biotoxins due to a lack of research studies in this field.
884 In other words, this field can advance biosensors and detoxification systems, managing biotoxin
885 threats in different environments and food matrices.

886 **Table 1.** Comparison reported of colorimetric sensors with nanozymes for detection of different
887 biotoxins.

Nanozymes	Enzyme activity	Substrate	Target	Linear range	LOD	Ref.
Au@HgNPs	OXD	TMB	AFB ₁	0.125 to 87.5 µg/L	0.08 µg/L	91
CHNPs	OXD	TMB	AFB ₁	1 pg/mL to 20 ng/mL	0.73 pg/mL	92
Au-Pt	OXD	TMB	AFB ₁	0.1 to 500 ng/mL	5 pg/mL	93
MoS ₂ /Au	POD	TMB	AFB ₁	1 to 100 ng/mL	0.25 ng/mL	141
Pt-CN	POD	TMB	AFB ₁	1.0 pg/mL to 10 ng/mL	0.22 pg/mL	95
Ag@Au IP6	POD	TMB	AFB ₁	2 pg/L to 200 pg/L	0.58 pg/L	98
MnO ₂ NSs	OXD	TMB	AFB ₁	0.01 to 150 ng/mL	0.015 ng/mL	99
CuCo@PDA	POD	TMB	AFB ₁	0.01 to 50 ng/mL	2.2 pg/mL	101
FeNiNPs	POD	TMB	AFB ₁	0.12 to 2 µg/mL	36.57 ng/mL	102
Pt@PCN-222	OXD	ABTS	AFB ₁	0.1 to 10 ng/mL	0.074 µg/L	142
NanoPCN-223	POD	TMB	AFB ₁	0.05 to 10 ng/mL	0.003 ng/mL	106
MnCo ₂ O ₄	OXD	TMB	OTA	0.1 to 10 ng/mL	0.08 ng/mL	111
Fe ₃ O ₄	POD	TMB	OTA	5 to 100 ng/mL	0.078 ng/mL	113
MnO ₂ NSs	OXD	TMB	OTA	1.25 to 250 nM	0.069 nM	115
Cu ₂ O nanocubes	OXD	TMB	OTA	0.5 ng/L to 5 mg/L	0.26 ng/L	116
Au@Pt	POD	TMB	Okadaic acid	0.8 to 6.8 ng/L	0.5 ng/L	119
AuNPs	POD	TMB	Saxitoxin	78.13 to 2500 pM	42.46 pM	120
AuNPs@Fe ²⁺	POD	TMB	Okadaic acid, dinophysistoxin-1, and dinophysistoxin-2	4688 to 7.5 nM	86.28 pM	123
Fe ₃ O ₄ @Au-Pt	OXD	TMB	Saxitoxin	0.01 to 100 µM	3.1 nM	126
AuNP/Co ₃ O ₄ @Mg/Al cLDH	POD	TMB	Saxitoxin	0 to 1000 ng/mL	3.17 ng/mL	127
Mn/Fe-MIL(53)@AuNSs	POD	TMB	Shiga toxin type II	0.05 to 500 ng/mL	26 pg/mL	130
AuPt@Fe-N-C	POD	TMB	<i>Staphylococcus aureus</i> enterotoxin B	0.0002 to 10.000 ng/mL	0667 pg/mL	131
Rh	POD	TMB	Staphylococcal enterotoxin B	0 to 2 ng/mL	1.2 pg/mL	132

888

889 6. Conclusions and future perspectives

890 Numerous attempts have been undertaken to control biotoxins; however, their contamination
891 remains largely inevitable. Therefore, there is an urgent need for research to explore the biosensors
892 for the rapid, sensitive, and convenient detection of biotoxins, given the detrimental impact of
893 biotoxins on human health and food safety. So, as described in this literature update, owing to their
894 favorable catalytic activity, excellent stability, and low cost, nanozymes and nanozyme-based
895 biosensors have been extensively exploited to identify different biotoxins in food and
896 environmental samples. In particular, the combination of colorimetric biosensors and nanozymes
897 to construct an innovative biosensing scaffold provides a promising outlook in convenient,
898 sensitive, and rapid quantification of various biotoxins. Herein, we discuss the production,
899 characteristics, and application of nanozymes in colorimetric biosensors, focusing on their diverse
900 catalytic activities. Furthermore, a comprehensive overview of the research conducted on the
901 utilization of nanozyme-based colorimetric biosensors for the identification of biotoxins is
902 provided. Through deliberating the sensing approaches employed by nanozyme-based colorimetric
903 biosensors, it becomes evident that these biosensors serve crucial roles in the rapid diagnosis of
904 biotoxins. Besides, we highlight the recent advancements in portable technologies, including
905 hydrogels and paper-based platforms, that can be integrated with smartphones to enable on-site
906 detection. Although nanozyme-based colorimetric biosensors possess the features of fast response,
907 simple operation, high sensitivity, and low cost, they still have some challenges in several aspects.

908 i) Due to the inferior catalytic efficiency of nanozymes in comparison with natural enzymes, the
909 application of nanozymes with multiple catalytic and high activity can be considered one of the
910 efficient strategies. Indeed, multiple catalytic including peroxidase-like, oxidase-like, and
911 catalase-like activities can improve the performance of nanozymes. Furthermore, the concept of

1
2
3
4
5
6
7
8
9
10
11
12
13
14
15
16
17
18
19
20
21
22
23
24
25
26
27
28
29
30
31
32
33
34
35
36
37
38
39
40
41
42
43
44
45
46
47
48
49
50
51
52
53
54
55
56
57
58
59
60

Open Access Article. Published on 09/10/2024. Downloaded on 09/10/2024 14:22:04.
This article is licensed under a Creative Commons Attribution-NonCommercial 3.0 Unported Licence.




1
2
3 912 high activate nanozymes is achieved by integration of nanozymes with different nanomaterials. As
4
5 913 well, the lower selectivity of nanozymes towards targets restricts specific recognition in the
6
7 914 detection process. Consequently, the development of novel nanozymes with enhanced specificity
8
9 915 could involve the integration of biomimetic recognition elements, such as MIPs, and exploring
10
11 916 additional technical approaches holds promise for future advancements in this area.
12
13

14
15 917 ii) Currently, an increasing number of studies are focusing on nanozymes exhibiting multiple
16
17 918 enzyme activities. However, the utilization of nanozymes with multiple enzyme performances in
18
19 919 colorimetric biosensors predominantly depends on their POD and OXD-like activities. Regulating
20
21 920 the predominant activity of nanozymes with multiple enzyme-like functions simultaneously poses
22
23 921 a significant challenge. This task necessitates a more precise comprehension of the catalytic
24
25 922 mechanisms underlying various enzyme activities, along with a thorough understanding of the
26
27 923 primary factors influencing these activities.
28
29

30
31 924 iii) The catalytic reactions occur in the specific regions on the nanozyme's surface which are
32
33 925 considered as active places. Generally, these active places are similarly operated based on the
34
35 926 active sites in natural enzymes. However, their function and structure can differ owing to the basic
36
37 927 differences between biological macromolecules and nanomaterials ¹⁴³. Elaborately, the presence
38
39 928 of a small number of amino acids can able natural enzymes to directly interact with the substrate.
40
41 929 Hydrophobic interactions and hydrogen bonding are the most important of these interactions,
42
43 930 providing the high efficiency and specificity substrate. On the other hand, specific atoms or
44
45 931 clusters of atoms on the surface of nanozymes act as active places. In detail, specific functional
46
47 932 groups or metal ions can mimic the catalytic functions of natural enzymes. In addition, the
48
49 933 chemical composition, size, and shape of nanozymes can impact on their catalytic activity ¹⁴⁴.
50
51
52
53
54 934

Open Access Article. Published on 09/10/2024. Downloaded on 09/10/2024. This article is licensed under a Creative Commons Attribution-NonCommercial 3.0 Unported Licence.



1
2
3 935 To sum up, the investigation of nanozymes and nanozyme-based colorimetric represents merely
4
5 936 the initial phase of a vast field of study. Nevertheless, it is evident that these biosensors exhibit
6
7 937 significant promise in applications and merit further investigation. As research on progresses and
8
9 938 nanozyme-based colorimetric biosensors continue to evolve, it is anticipated that more cutting-
10
11 939 edge technologies and portable devices will be developed and extensively employed to safeguard
12
13 940 food and environmental integrity.


941 **Acknowledgments**

942 This work was financially supported by Jiyang College of Zhejiang A&F University (RQ1911F12)
943 and Scientific Research Project of Education Department of Zhejiang Province (Y202352649).

944 **References**

- 945 1. M. Mahmoudpour, J. Ezzati Nazhad Dolatabadi, M. Torbati, A. Pirpour Tazehkand, A.
946 Homayouni-Rad and M. de la Guardia, *Biosensors and Bioelectronics*, 2019, **143**, 111603.
- 947 2. M. Mahmoudpour, J. Ezzati Nazhad Dolatabadi, M. Torbati and A. Homayouni-Rad, *Biosensors*
948 *and Bioelectronics*, 2019, **127**, 72-84.
- 949 3. J. Nicolas, R. L. Hoogenboom, P. J. Hendriksen, M. Boder, T. F. Bovee, I. M. Rietjens and A.
950 Gerssen, *Global Food Security*, 2017, **15**, 11-21.
- 951 4. M.-L. Liu, X.-M. Liang, M.-Y. Jin, H.-W. Huang, L. Luo, H. Wang, X. Shen and Z.-L. Xu, *Journal of*
952 *Agricultural and Food Chemistry*, 2024.
- 953 5. F. Javaheri-Ghezeldizaj, M. Mahmoudpour, R. Yekta and J. Ezzati Nazhad Dolatabadi, *Journal of*
954 *Molecular Liquids*, 2020, **310**, 113259.
- 955 6. C. Lin, Z.-S. Liu, C.-Y. Tan, Y.-P. Guo, L. Li, H.-L. Ren, Y.-S. Li, P. Hu, S. Gong and Y. Zhou,
956 *Environmental Science and Pollution Research*, 2015, **22**, 1545-1553.
- 957 7. D. Liu, in *Molecular Medical Microbiology*, Elsevier, 2024, pp. 933-944.
- 958 8. P. Sadeghi, H. Sohrabi, M. R. Majidi, A. Eftekhari, F. Zargari, M. de la Guardia and A. A.
959 Mokhtarzadeh, *TrAC Trends in Analytical Chemistry*, 2024, 117722.
- 960 9. Y. Liu and F. Wu, *Environmental health perspectives*, 2010, **118**, 818-824.
- 961 10. S. Siva, J.-O. Jin, I. Choi and M. Kim, *Biosensors and Bioelectronics*, 2023, **219**, 114845.
- 962 11. M. Mahmoudpour, S. Ding, Z. Lyu, G. Ebrahimi, D. Du, J. Ezzati Nazhad Dolatabadi, M. Torbati
963 and Y. Lin, *Nano Today*, 2021, **39**, 101177.
- 964 12. Z. Karimzadeh, M. Mahmoudpour, E. Rahimpour and A. Jouyban, *Advances in Colloid and*
965 *Interface Science*, 2022, **305**, 102705.
- 966 13. T. A. Rocha-Santos, *TrAC Trends in Analytical Chemistry*, 2014, **62**, 28-36.
- 967 14. Z. Golsanamlou, M. Mahmoudpour, J. Soleymani and A. Jouyban, *Critical Reviews in Analytical*
968 *Chemistry*, 2023, **53**, 1116-1131.
- 969 15. Z. Khoshbin, M. Moeenfard, K. Abnous and S. M. Taghdisi, *Food Chemistry*, 2024, **433**, 137355.

Open Access Article. Published on 20/09/2024. Downloaded on 20/09/2024. This article is licensed under a Creative Commons Attribution 3.0 Unported Licence.



- 1
2
3 970 16. L. Lu, R. Yu and L. Zhang, *Food Chemistry*, 2023, **421**, 136205.
4 971 17. R. L. F. Melo, F. S. Neto, D. N. Dari, B. C. C. Fernandes, T. M. Freire, P. B. A. Fechine, J. M. Soares
5 972 and J. C. S. Dos Santos, *International Journal of Biological Macromolecules*, 2024, 130817.
6 973 18. T. Vyas, V. Singh, P. Kodgire and A. Joshi, *Critical Reviews in Biotechnology*, 2023, **43**, 521-539.
7 974 19. J. Qin, N. Guo, J. Yang and J. Wei, *Food Chemistry*, 2024, 139019.
8 975 20. A. Baranwal, R. Shukla and V. Bansal, *TrAC Trends in Analytical Chemistry*, 2024, 117573.
9 976 21. L. Yang, X. Xu, Y. Song, J. Huang and H. Xu, *Chemical Engineering Journal*, 2024, **487**, 150612.
10 977 22. Z. Chi, Q. Wang and J. Gu, *Analyst*, 2023, **148**, 487-506.
11 978 23. B. Unnikrishnan, C.-W. Lien, H.-W. Chu and C.-C. Huang, *Journal of Hazardous Materials*, 2021,
12 979 **401**, 123397.
13 980 24. Y. Huang, J. Ren and X. Qu, *Chemical reviews*, 2019, **119**, 4357-4412.
14 981 25. H. Wei, L. Gao, K. Fan, J. Liu, J. He, X. Qu, S. Dong, E. Wang and X. Yan, *Nano Today*, 2021, **40**,
15 982 101269.
16 983 26. L. Zhang, H. Wang and X. Qu, *Advanced Materials*, 2024, **36**, 2211147.
17 984 27. Z. Li, W. Liu, P. Ni, C. Zhang, B. Wang, G. Duan, C. Chen, Y. Jiang and Y. Lu, *Chemical Engineering*
18 985 *Journal*, 2022, **428**, 131396.
19 986 28. Z. Lou, S. Zhao, Q. Wang and H. Wei, *Analytical chemistry*, 2019, **91**, 15267-15274.
20 987 29. K. Fan, J. Xi, L. Fan, P. Wang, C. Zhu, Y. Tang, X. Xu, M. Liang, B. Jiang and X. Yan, *Nature*
21 988 *Communications*, 2018, **9**, 1440.
22 989 30. P. Zhang, D. Sun, A. Cho, S. Weon, S. Lee, J. Lee, J. W. Han, D.-P. Kim and W. Choi, *Nature*
23 990 *communications*, 2019, **10**, 940.
24 991 31. S. Pandit and M. De, *Nanoscale Advances*, 2021, **3**, 5102-5110.
25 992 32. H. Sun, A. Zhao, N. Gao, K. Li, J. Ren and X. Qu, *Angewandte Chemie International Edition*, 2015,
26 993 **54**, 7176-7180.
27 994 33. M. Mahmoudpour, J. E. N. Dolatabadi, M. Hasanzadeh, A. H. Rad, M. Torbati and F. Seidi, *RSC*
28 995 *advances*, 2022, **12**, 29602-29612.
29 996 34. M. S. Kim, S. Cho, S. H. Joo, J. Lee, S. K. Kwak, M. I. Kim and J. Lee, *ACS nano*, 2019, **13**, 4312-
30 997 4321.
31 998 35. Z. Wang, Z. Xu, X. Xu, J. Xi, J. Han, L. Fan and R. Guo, *Colloids and Surfaces B: Biointerfaces*, 2022,
32 999 **217**, 112671.
33 1000 36. F. Li, J. Jiang, H. Peng, C. Li, B. Li and J. He, *Sensors and Actuators B: Chemical*, 2022, **369**,
34 1001 132334.
35 1002 37. L. Zhu, W. Zeng, Y. Li, Y. Han, J. Wei and L. Wu, *Science of The Total Environment*, 2024, **921**,
36 1003 171236.
37 1004 38. X. Liang, X. Wang, Y. Zhang, B. Huang and L. Han, *Journal of Agricultural and Food Chemistry*,
38 1005 2022, **70**, 3898-3906.
39 1006 39. X. Zhang, Y. Xu, X. Wang, T. Chen, Q. Yao, S. Chang, X. Guo, X. Liu, H. Wu and Y. Cui, *Food*
40 1007 *Chemistry*, 2024, 140710.
41 1008 40. C. Lu, L. Tang, F. Gao, Y. Li, J. Liu and J. Zheng, *Biosensors and Bioelectronics*, 2021, **187**, 113327.
42 1009 41. S. Naveen Prasad, P. Weerathunge, M. N. Karim, S. Anderson, S. Hashmi, P. D. Mariathomas, V.
43 1010 Bansal and R. Ramanathan, *Analytical and Bioanalytical Chemistry*, 2021, **413**, 1279-1291.
44 1011 42. D. Li, D. Dai, G. Xiong, S. Lan and C. Zhang, *Small*, 2023, **19**, 2205870.
45 1012 43. P. T. Nguyen, J. Lee, A. Cho, M. S. Kim, D. Choi, J. W. Han, M. I. Kim and J. Lee, *Advanced*
46 1013 *Functional Materials*, 2022, **32**, 2112428.
47 1014 44. Y. Lin, C. Xu, J. Ren and X. Qu, *Angewandte Chemie (International ed. in English)*, 2012, **51**,
48 1015 12579-12583.
49 1016 45. L. Gao, J. Zhuang, L. Nie, J. Zhang, Y. Zhang, N. Gu, T. Wang, J. Feng, D. Yang and S. Perrett,
50 1017 *Nature nanotechnology*, 2007, **2**, 577-583.



- 1
2
3 1018 46. R. André, F. Natálio, M. Humanes, J. Leppin, K. Heinze, R. Wever, H. C. Schröder, W. E. Müller
4 1019 and W. Tremel, *Advanced Functional Materials*, 2011, **21**, 501-509.
5 1020 47. A. B. Ganganboina and R.-a. Doong, *Sensors and Actuators B: Chemical*, 2018, **273**, 1179-1186.
6 1021 48. H. Li, S. Zhao, Z. Wang and F. Li, *Small*, 2023, **19**, 2206465.
7 1022 49. L. Han, H. Zhang, D. Chen and F. Li, *Advanced Functional Materials*, 2018, **28**, 1800018.
8 1023 50. Q. Liu, A. Zhang, R. Wang, Q. Zhang and D. Cui, *Nano-micro letters*, 2021, **13**, 1-53.
9 1024 51. Z. Karimzadeh, M. Mahmoudpour, M. d. I. Guardia, J. Ezzati Nazhad Dolatabadi and A. Jouyban,
10 1025 *TrAC Trends in Analytical Chemistry*, 2022, **152**, 116622.
11 1026 52. Z. Karimzadeh, M. Mahmoudpour, E. Rahimpour and A. Jouyban, *RSC advances*, 2024, **14**, 9571-
12 1027 9586.
13 1028 53. Z. Karimzadeh, A. Jouyban, A. Ostadi, A. Gharakhani and E. Rahimpour, *Analytica Chimica Acta*,
14 1029 2022, **1227**, 340252.
15 1030 54. X. Zhang, G. Li, D. Wu, X. Li, N. Hu, J. Chen, G. Chen and Y. Wu, *Biosensors and Bioelectronics*,
16 1031 2019, **137**, 178-198.
17 1032 55. X. Huang, S. Zhang, Y. Tang, X. Zhang, Y. Bai and H. Pang, *Coordination Chemistry Reviews*, 2021,
18 1033 **449**, 214216.
19 1034 56. W. He, Z. Li, S. Lv, M. Niu, W. Zhou, J. Li, R. Lu, H. Gao, C. Pan and S. Zhang, *Chemical Engineering*
20 1035 *Journal*, 2021, **409**, 128274.
21 1036 57. K. Zhang, K. Dai, R. Bai, Y. Ma, Y. Deng, D. Li, X. Zhang, R. Hu and Y. Yang, *Chinese Chemical*
22 1037 *Letters*, 2019, **30**, 664-667.
23 1038 58. Z. Sun, M. Wang, J. Fan, R. Feng, Y. Zhou and L. Zhang, *Advanced Composites and Hybrid*
24 1039 *Materials*, 2021, **4**, 1322-1329.
25 1040 59. Y. Su, M. Lu, R. Su, W. Zhou, X. Xu and Q. Li, *Chinese Chemical Letters*, 2022, **33**, 2573-2578.
26 1041 60. L. Zheng, F. Wang, C. Jiang, S. Ye, J. Tong, P. Dramou and H. He, *Coordination Chemistry Reviews*,
27 1042 2022, **471**, 214760.
28 1043 61. X. Niu, B. Liu, P. Hu, H. Zhu and M. Wang, *Biosensors*, 2022, **12**, 251.
29 1044 62. H. Deng, Y. Zhang, X. Cai, Z. Yin, Y. Yang, Q. Dong, Y. Qiu and Z. Chen, *Small*, 2024, **20**, 2306155.
30 1045 63. Z. Wang, M. Li, H. Bu, D. S. Zia, P. Dai and J. Liu, *Materials Chemistry Frontiers*, 2023, **7**, 3625-
31 1046 3640.
32 1047 64. M.-L. Ye, Y. Zhu, Y. Lu, L. Gan, Y. Zhang and Y.-G. Zhao, *Talanta*, 2021, **230**, 122299.
33 1048 65. Y. Song, K. Qu, C. Zhao, J. Ren and X. Qu, *Advanced Materials*, 2010, **22**, 2206-2210.
34 1049 66. Z. Lyu, J. Zhou, S. Ding, D. Du, J. Wang, Y. Liu and Y. Lin, *TrAC Trends in Analytical Chemistry*,
35 1050 2023, 117280.
36 1051 67. X. Zhang, C. Sun, R. Li, X. Jin, Y. Wu and F. Fu, *Analytical Chemistry*, 2023, **95**, 5024-5033.
37 1052 68. H. Li, M. Sun, H. Gu, J. Huang, G. Wang, R. Tan, R. Wu, X. Zhang, S. Liu and L. Zheng, *Small*, 2023,
38 1053 **19**, 2207036.
39 1054 69. M. Comotti, C. Della Pina, R. Matarrese and M. Rossi, *Angewandte Chemie International Edition*,
40 1055 2004, **43**, 5812-5815.
41 1056 70. Y. Peng, M. Huang, L. Chen, C. Gong, N. Li, Y. Huang and C. Cheng, *Nano Research*, 2022, **15**,
42 1057 8783-8790.
43 1058 71. M. Ren, Y. Zhang, L. Yu, L. Qu, Z. Li and L. Zhang, *Talanta*, 2023, **255**, 124219.
44 1059 72. X. Zhou, M. Wang, J. Chen and X. Su, *Talanta*, 2022, **245**, 123451.
45 1060 73. S. Khajir, Z. Karimzadeh, M. Khoubnasabjafari, V. Jouyban-Gharamaleki, E. Rahimpour and A.
46 1061 Jouyban, *Journal of Pharmaceutical and Biomedical Analysis*, 2023, **223**, 115141.
47 1062 74. S. Singh, *Frontiers in chemistry*, 2019, **7**, 46.
48 1063 75. S. Singh, *International Journal of Biological Macromolecules*, 2024, 129374.
49 1064 76. D. Mehta, P. Sharma and S. Singh, *Colloids and Surfaces B: Biointerfaces*, 2023, **231**, 113531.
50 1065 77. M. S. Lord, J. F. Berret, S. Singh, A. Vinu and A. S. Karakoti, *Small*, 2021, **17**, 2102342.
51
52
53
54
55
56
57
58
59
60

- 1
2
3 1066 78. A. K. Singh, K. Bijalwan, N. Kaushal, A. Kumari, A. Saha and A. Indra, *ACS Applied Nano Materials*,
4 1067 2023, **6**, 8036-8045.
5 1068 79. M. Zhang, Y. Wang, N. Li, D. Zhu and F. Li, *Biosensors and Bioelectronics*, 2023, **237**, 115554.
6 1069 80. M. Jia, F. Xu, F. Zhai, X. Yu and M. Du, *Journal of Colloid and Interface Science*, 2024, **653**, 1805-
7 1070 1816.
8 1071 81. C. P. Liu, T. H. Wu, C. Y. Liu, K. C. Chen, Y. X. Chen, G. S. Chen and S. Y. Lin, *Small*, 2017, **13**,
9 1072 1700278.
10 1073 82. S. Guo, Y. Han and L. Guo, *Catalysis Surveys from Asia*, 2020, **24**, 70-85.
11 1074 83. Z. Wang, X. Shen, X. Gao and Y. Zhao, *Nanoscale*, 2019, **11**, 13289-13299.
12 1075 84. R. Zhang, B. Xue, Y. Tao, H. Zhao, Z. Zhang, X. Wang, X. Zhou, B. Jiang, Z. Yang and X. Yan,
13 1076 *Advanced Materials*, 2022, **34**, 2205324.
14 1077 85. W. Yang, X. Yang, L. Zhu, H. Chu, X. Li and W. Xu, *Coordination Chemistry Reviews*, 2021, **448**,
15 1078 214170.
16 1079 86. A. Casu, M. Camardo Leggieri, P. Toscano and P. Battilani, *Comprehensive Reviews in Food*
17 1080 *Science and Food Safety*, 2024, **23**, e13323.
18 1081 87. M.-H. Moosavy, M. Hasanzadeh, J. Soleymani and A. Mokhtarzadeh, *Analytical methods*, 2019,
19 1082 **11**, 3910-3919.
20 1083 88. Y. Zhang, X. Chen, X. Xie, D. Li, Y. Fan, B. Huang and X. Yang, *Current Analytical Chemistry*, 2024,
21 1084 **20**, 242-254.
22 1085 89. Z. Xue, Y. Zhang, W. Yu, J. Zhang, J. Wang, F. Wan, Y. Kim, Y. Liu and X. Kou, *Analytica chimica*
23 1086 *acta*, 2019, **1069**, 1-27.
24 1087 90. C. Peng, R. Pang, J. Li and E. Wang, *Advanced Materials*, 2024, **36**, 2211724.
25 1088 91. X. Zhao, Q. Li, H. Li, Y. Wang, F. Xiao, D. Yang, Q. Xia and Y. Yang, *Food Chemistry*, 2023, **424**,
26 1089 136443.
27 1090 92. W. Lai, J. Guo, Y. Wang, Y. Lin, S. Ye, J. Zhuang and D. Tang, *Talanta*, 2022, **247**, 123546.
28 1091 93. L. Wu, M. Zhou, Y. Wang and J. Liu, *Journal of hazardous materials*, 2020, **399**, 123154.
29 1092 94. W. Jiang, Q. Yang, H. Duo, W. Wu and X. Hou, *Food Chemistry*, 2024, 138917.
30 1093 95. S. Huang, W. Lai, B. Liu, M. Xu, J. Zhuang, D. Tang and Y. Lin, *Spectrochimica Acta Part A:*
31 1094 *Molecular and Biomolecular Spectroscopy*, 2023, **284**, 121782.
32 1095 96. N. Ullah, T. A. Bruce-Tagoe, G. A. Asamoah and M. K. Danquah, *International Journal of*
33 1096 *Molecular Sciences*, 2024, **25**, 5959.
34 1097 97. S. Ganguly and S. Margel, *Talanta Open*, 2023, 100243.
35 1098 98. X. Tan, K. Kang, R. Zhang, J. Dong, W. Wang and W. Kang, *Sensors and Actuators B: Chemical*,
36 1099 2024, **412**, 135854.
37 1100 99. X. Cai, M. Liang, F. Ma, Z. Zhang, X. Tang, J. Jiang, C. Guo, S. R. Mohamed, A. A. Goda and D. H.
38 1101 Dawood, *Food Chemistry*, 2022, **377**, 131965.
39 1102 100. T. Bu, P. Jia, X. Sun, Y. Liu, Q. Wang and L. Wang, *Sensors and Actuators B: Chemical*, 2020, **320**,
40 1103 128440.
41 1104 101. X. Zhu, J. Tang, X. Ouyang, Y. Liao, H. Feng, J. Yu, L. Chen, Y. Lu, Y. Yi and L. Tang, *Journal of*
42 1105 *Hazardous Materials*, 2024, **465**, 133178.
43 1106 102. Y. Fan, D. Li, X. Xie, Y. Zhang, L. Jiang, B. Huang and X. Yang, *Microchemical Journal*, 2024, **197**,
44 1107 109842.
45 1108 103. X. Zhang, M. C. Wasson, M. Shayan, E. K. Berdichevsky, J. Ricardo-Noordberg, Z. Singh, E. K.
46 1109 Papazyan, A. J. Castro, P. Marino and Z. Ajoyan, *Coordination chemistry reviews*, 2021, **429**,
47 1110 213615.
48 1111 104. P. Li, R. C. Klet, S.-Y. Moon, T. C. Wang, P. Deria, A. W. Peters, B. M. Klahr, H.-J. Park, S. S. Al-
49 1112 Juaid and J. T. Hupp, *Chemical communications*, 2015, **51**, 10925-10928.
50 1113 105. S. Zhang, H. Li, Q. Xia, D. Yang and Y. Yang, *Journal of Food Science*, 2024.



- 1
2
3 1114 106. S. Peng, K. Li, Y.-x. Wang, L. Li, Y.-H. Cheng and Z. Xu, *Analytical Biochemistry*, 2022, **655**, 114829.
4 1115 107. C. Jiang, L. Lan, Y. Yao, F. Zhao and J. Ping, *TrAC Trends in Analytical Chemistry*, 2018, **102**, 236-
5 1116 249.
6 1117 108. Y. Alhamoud, D. Yang, S. S. F. Kenston, G. Liu, L. Liu, H. Zhou, F. Ahmed and J. Zhao, *Biosensors
7 1118 and Bioelectronics*, 2019, **141**, 111418.
8 1119 109. Q. Zhao, Z. Yan, C. Chen and J. Chen, *Chemical reviews*, 2017, **117**, 10121-10211.
9 1120 110. L. Gao, K. Fan and X. Yan, *Nanozymology: Connecting Biology and Nanotechnology*, 2020, 105-
10 1121 140.
11 1122 111. L. Huang, K. Chen, W. Zhang, W. Zhu, X. Liu, J. Wang, R. Wang, N. Hu, Y. Suo and J. Wang,
12 1123 *Sensors and Actuators B: Chemical*, 2018, **269**, 79-87.
13 1124 112. J. M. Gonçalves, L. V. de Faria, A. B. Nascimento, R. L. Germscheidt, S. Patra, L. P. Hernández-
14 1125 Saravia, J. A. Bonacin, R. A. Munoz and L. Angnes, *Analytica Chimica Acta*, 2022, **1233**, 340362.
15 1126 113. Q. Liu, S. Xin, X. Tan, Q. Yang and X. Hou, *Microchimica Acta*, 2023, **190**, 364.
16 1127 114. M. K. Masud, J. Kim, M. M. Billah, K. Wood, M. J. Shiddiky, N.-T. Nguyen, R. K. Parsapur, Y. V.
17 1128 Kaneti, A. A. Alshehri and Y. G. Alghamidi, *Journal of materials chemistry B*, 2019, **7**, 5412-5422.
18 1129 115. F. Tian, J. Zhou, B. Jiao and Y. He, *Nanoscale*, 2019, **11**, 9547-9555.
19 1130 116. H. Zhu, Z. Quan, H. Hou, Y. Cai, W. Liu and Y. Liu, *Analytica Chimica Acta*, 2020, **1132**, 101-109.
20 1131 117. L. Zhao, H. Guo, H. Chen, B. Zou, C. Yang, X. Zhang, Y. Gao, M. Sun and L. Wang, *Bioengineering*,
21 1132 2022, **9**, 684.
22 1133 118. H. kholafazad Kordasht, S. Hassanpour, B. Baradaran, R. Nosrati, M. Hashemzaei, A.
23 1134 Mokhtarzadeh and M. de la Guardia, *Biosensors and Bioelectronics*, 2020, **165**, 112403.
24 1135 119. O. D. Hendrickson, E. A. Zvereva, V. G. Panferov, O. N. Solopova, A. V. Zherdev, P. G. Sveshnikov
25 1136 and B. B. Dzantiev, *Biosensors*, 2022, **12**, 1137.
26 1137 120. Y. Zhao, L. Li, R. Ma, L. Wang, X. Yan, X. Qi, S. Wang and X. Mao, *Analytica Chimica Acta*, 2021,
27 1138 **1173**, 338710.
28 1139 121. X. Qi, L. Li, X. Yan, Y. Zhao, L. Wang, R. Ma, S. Wang and X. Mao, *Journal of Ocean University of
29 1140 China*, 2022, **21**, 1343-1350.
30 1141 122. S. Wang, Y. Zhao, R. Ma, W. Wang, L. Zhang, J. Li, J. Sun and X. Mao, *Food Chemistry*, 2023, **401**,
31 1142 134053.
32 1143 123. L. Li, R. Ma, Y. Zhao, L. Wang, S. Wang and X. Mao, *Talanta*, 2022, **246**, 123534.
33 1144 124. F. Cui, Z. Zhou and H. S. Zhou, *Sensors*, 2020, **20**, 996.
34 1145 125. J. Marfà, R. Pupin, M. Sotomayor and M. Pividori, *Analytical and Bioanalytical Chemistry*, 2021,
35 1146 **413**, 6141-6157.
36 1147 126. L. Wu, Y. Li, Y. Han, X. Liu, B. Han, H. Mao and Q. Chen, *Journal of Food Composition and
37 1148 Analysis*, 2024, **130**, 106190.
38 1149 127. C. H. Cho, J. H. Kim, N. S. Padalkar, Y. V. M. Reddy, T. J. Park, J. Park and J. P. Park, *Biosensors and
39 1150 Bioelectronics*, 2024, **255**, 116269.
40 1151 128. C. Hernández-Cortez, I. Palma-Martínez, L. U. Gonzalez-Avila, A. Guerrero-Mandujano, R. C. Solís
41 1152 and G. Castro-Escarpulli, *Poisoning: From specific toxic agents to novel rapid and simplified
42 1153 techniques for analysis*, 2017, **33**.
43 1154 129. R. Gupta, N. Raza, S. K. Bhardwaj, K. Vikrant, K.-H. Kim and N. Bhardwaj, *Journal of hazardous
44 1155 materials*, 2021, **401**, 123379.
45 1156 130. K. Ren, M. Duan, T. Su, D. Ying, S. Wu, Z. Wang and N. Duan, *Talanta*, 2024, **270**, 125636.
46 1157 131. H. Liang, H. Liu, H. Lin, G. Ning, X. Lu, S. Ma, F. Liu, H. Zhao and C. Li, *Food Science and Human
47 1158 Wellness*, 2024, **13**, 2025-2035.
48 1159 132. X. Cai, Y. Luo, C. Zhu, D. Huang and Y. Song, *Sensors and Actuators B: Chemical*, 2022, **367**,
49 1160 132066.
50
51
52
53
54
55
56
57
58
59
60

- 1
2
3 1161 133. Y. Xing, F. Yasinjan, S. Sun, J. Yang, Y. Du, H. Zhang, Y. Liang, H. Geng, Y. Wang and J. Sun, *Nano*
4 1162 *Today*, 2024, **57**, 102386.
5 1163 134. D. Li, T. Fan and X. Mei, *Nanoscale*, 2023, **15**, 15885-15905.
6 1164 135. Q. Lu, Q. Li, Y. An, X. Duan, R. Zhao, D. Zhao and S. An, *Journal of Cleaner Production*, 2022, **376**,
7 1165 134117.
8 1166 136. M. Tudi, H. Daniel Ruan, L. Wang, J. Lyu, R. Sadler, D. Connell, C. Chu and D. T. Phung,
9 1167 *International journal of environmental research and public health*, 2021, **18**, 1112.
10 1168 137. M. Song, University of Nevada, Reno, 2022.
11 1169 138. N. K. V. Leitner, in *Advanced oxidation processes for water treatment: fundamentals and*
12 1170 *applications*, IWA Publishing, 2017, pp. 429-460.
13 1171 139. Z. A. Mohamed, Y. Mostafa, S. Alamri, M. Hashem and S. Alrumman, 2022.
14 1172 140. X. Yang, J. Pan, J. Hu, S. Zhao and K. Cheng, *Chemical Engineering Journal*, 2023, **467**, 143381.
15 1173 141. W. Jiang, Q. Yang, H. Duo, W. Wu and X. Hou, *Food Chemistry*, 2024, **447**, 138917.
16 1174 142. S. Zhang, H. Li, Q. Xia, D. Yang and Y. Yang, *Journal of Food Science*, 2024, **89**, 3618-3628.
17 1175 143. R. Zhang, X. Yan and K. Fan, *Accounts of Materials Research*, 2021, **2**, 534-547.
18 1176 144. Y. Chong, Q. Liu and C. Ge, *Nano Today*, 2021, **37**, 101076.

1177

1178

1179

1180

1181

1182

1183


1184

1185

1186

1187

Open Access Article. Published on 09/10/2024. Downloaded on 20/10/2024 14:22:04.
This article is licensed under a Creative Commons Attribution 3.0 Unported Licence.



Data availability

No data was used for the research described in the article.

1
2
3
4
5
6
7
8
9
10
11
12
13
14
15
16
17
18
19
20
21
22
23
24
25
26
27
28
29
30
31
32
33
34
35
36
37
38
39
40
41
42
43
44
45
46
47
48
49
50
51
52
53
54
55
56
57
58
59
60

Open Access Article. Published on 09/10/2024. Downloaded on 09/10/2024. This article is licensed under a Creative Commons Attribution-NonCommercial 3.0 Unported Licence.



Analytical Methods Accepted Manuscript